

Slip and Jump Coefficients for General Gas-Surface Interactions According to the Moment Method

Ruo Li* Yichen Yang†

January 31, 2023

Abstract

We develop a moment method based on the Hermite series of arbitrary order to calculate viscous-slip, thermal-slip, and temperature-jump coefficients for general gas-surface scattering kernels. Under some usual assumptions of scattering kernels, the solvability is obtained by showing the positive definiteness of the symmetric coefficient matrix in the boundary conditions. For gas flows with the Cercignani-Lampis gas-surface interaction and inverse-power-law intermolecular potentials, the model can capture the slip and jump coefficients accurately with elegant analytic expressions. On the one hand, the proposed method can apply to the cases of arbitrary order moments with increasing accuracy. On the other hand, the explicit formulae for low-order situations are simpler and more accurate than some existing results in references. Therefore, one may apply these formulae in slip and jump conditions to improve the accuracy of macroscopic fluid dynamic models for gas flows.

1 Introduction

The rarefied gas flow effects such as the velocity slip, temperature jump, and thermally induced flows near the solid wall, are fundamental issues in micro-electro-mechanical systems (MEMS) and low-density hypersonic aerodynamics. [14, 8, 51, 1] The rarefaction is often measured by the Knudsen number, i.e., the ratio of the mean free path to the characteristic length. As the Knudsen number goes larger, the continuum assumption breaks down, and the traditional Navier-Stokes equations are no longer applicable. One may impose slip and jump boundary conditions to enlarge the application scope of the Navier-Stokes equations, where the slip and jump coefficients play a crucial role in the accuracy of the macroscopic fluid dynamic equations. [44, 1]

From a statistical standpoint, the Boltzmann equation can describe the rarefied gas flows, with a general scattering kernel to specify the gas-surface interaction. [9] The most popular scattering kernel may be the Maxwell diffuse-specular kernel, which has one accommodation coefficient (AC) to parameterize the roughness of the solid wall. However, as shown in experiments and molecular dynamics (MD) simulations, [49, 44, 35] the Maxwell model with a single AC is inadequate to capture all the scattering behavior of the reflected molecules. Alternatively, the classical Cercignani-Lampis (CL) scattering kernel [10] has two ACs individually measuring the exchange of tangential momentum and normal energy. The CL boundary conditions (BCs) are more realistic and agree well with some experimental and MD data. [41, 2]

Due to the extreme importance of slip and jump coefficients, many theoretical and numerical efforts have been paid to study these issues, especially for general gas-surface interactions beyond the Maxwell model. Slip and jump coefficients can be obtained from half-space layer equations [3, 37, 4] that depict the boundary behavior of the rarefied gas flows. The corresponding explicit expressions in terms of a set ACs have been given by the variational principle [11, 22, 27, 33] and the low-order moment-type methods. These moment methods usually assume the velocity distribution

*CAPT, LMAM & School of Mathematical Sciences, Peking University, Beijing 100871, China, email: rli@math.pku.edu.cn.

†School of Mathematical Sciences, Peking University, Beijing 100871, China, email: yichenyang@pku.edu.cn.

function to be a Maxwellian multiplied by low-order polynomials. For the Maxwell diffuse-specular BCs, there are some famous moment-type methods such as the Maxwell method, [32] the Loyalka method, [29] and the half-range moment method. [18] Similar ideas have been applied to the CL BCs. [39, 50] There are direct numerical methods to calculate slip and jump coefficients. In contrast to the Maxwell model, [35] fewer data are available for the CL BCs. Siewert has developed an analytical discrete-ordinates method to numerically solve the layer problems based on the linearized Boltzmann equation (LBE). [36] Note that the above work is all restricted to the simplified collision models or the hard-sphere potential. For general intermolecular potentials, the LBE is directly solved by a synthetic iteration scheme and fast spectral method recently to predict slip and jump coefficients. [41, 45, 40]

The paper will focus on the Grad moment method [16] based on the arbitrary order Hermite expansion of the velocity distribution function. The Grad-type moment model with 13 moments, [43, 42] 26 moments, [19, 20] and an arbitrary number of moments [38, 13, 24] have been developed to study the slip and jump. It's promising that the accuracy of the moment model can improve when we enlarge the number of used moments. However, the related theory is mainly on the Maxwell BCs, and the numerical results are mostly reported for simplified collision models. Here, we develop the arbitrary order moment method to model the layer problems with general BCs. In particular, we achieve the numerical solutions and explicit formulae of slip and jump coefficients for the CL BCs and inverse-power-law (IPL) intermolecular potentials.

There are three distinct difficulties when we extend the moment methods to general cases. Firstly, although the general mathematical formulation of the layer problems based on the LBE is well-known, [48, 36] it's hard to find a clear and rigorous definition of the layer problems for the moment method with arbitrary order and IPL potentials. Secondly, the solvability of the layer equations is not for granted. The general well-posed theory of the boundary value problem for the moment equations are studied in Ref.[24, 25]. Similar results about the discrete Boltzmann equation are given in Ref.[4, 6, 5]. We need to verify the solvability conditions for the moment equations with general BCs. Thirdly, the numerical treatment of the layer equations with general BCs is not trivial. The calculation of the IPL potentials has been recently considered in Ref.[46]. The Hermite expansion of the CL scattering kernel is mainly a two-dimensional half-space integral, which is a combination of the modified Bessel function, Hermite polynomials, exponentials, and powers. The reckless numerical integration may bring considerable errors and prevent us from finding explicit expressions of slip and jump coefficients in terms of the ACs.

The paper is devoted to all of the above issues. We define the layer problems based on the moment method with arbitrary order according to the spirit of the Chapman-Enskog expansion. The model can depict all classical half-space problems with IPL potentials. To ensure the solvability, we make a careful choice of the test functions and the simple boundary stabilization with a rank-one modification. Briefly speaking, the rank-one modification removes the eigenvalue one arising from the normalization property of the scattering kernel, which leads to the positive definiteness of the symmetric coefficient matrix. To obtain explicit formulae, we give closed-form integral representations involving the CL scattering kernel and Hermite polynomials by a recursion relation. These formulae explain the influence of the two ACs in the CL kernel and the different intermolecular potentials.

The rest of this paper is organized as follows. In Section 2, we briefly review the layer equations and derive the general BCs for them. In Section 3, we verify the solvability of the layer equations. In Section 4, we focus on the calculation of the CL scattering kernel. In Section 5, we consider the specific half-space problems. We give highly accurate numerical results and explicit formulae about slip and jump coefficients. The paper ends with conclusions.

2 The Moment Model

2.1 Review on the layer equations

For single-species monatomic gases, the half-space equations for the moment model read as [13, 24]

$$\begin{aligned} \mathbf{A}_2 \frac{d\mathbf{w}}{dy} &= -\mathbf{Q}\mathbf{w}, \quad \mathbf{w} = \mathbf{w}(y), \quad y \in [0, +\infty), \\ \mathbf{w}(\infty) &= \mathbf{0}, \end{aligned} \quad (1)$$

where $\mathbf{w} = \mathbf{w}(y) \in \mathbb{R}^N$ is the moment variable in the Knudsen layer and \mathbf{A}_2 as well as \mathbf{Q} are constant matrices. The argument y is the stretched coordinate normal to the boundary. This class of half-space equations can depict the boundary behavior of the rarefied gas flows. [3, 37, 4]

The moment variable is from the Hermite series of the velocity distribution function. Let $\omega = \omega(\boldsymbol{\xi})$ be the global Maxwellian

$$\omega(\boldsymbol{\xi}) = (2\pi)^{-3/2} \exp(-|\boldsymbol{\xi}|^2/2), \quad (2)$$

where $\boldsymbol{\xi} = (\xi_1, \xi_2, \xi_3) \in \mathbb{R}^3$ is the microscopic velocity of particles. The corresponding Hermite polynomials $\phi_\alpha = \phi_\alpha(\boldsymbol{\xi})$ are defined [15] by the recursion relation

$$\xi_d \phi_\alpha = \sqrt{\alpha_d} \phi_{\alpha - e_d} + \sqrt{\alpha_d + 1} \phi_{\alpha + e_d}, \quad \alpha = (\alpha_1, \alpha_2, \alpha_3) \in \mathbb{N}^3, \quad (3)$$

where $\phi_{\mathbf{0}} = 1$ and $\phi_{e_i} = \xi_i$, with $e_i \in \mathbb{N}^3$ only the i -th element being one. As a convention, we regard ϕ_α as zero if any component of α is negative. Then we have the orthogonality

$$\langle \omega \phi_\alpha \phi_\beta \rangle = \delta_{\alpha, \beta}, \quad \langle \cdot \rangle \triangleq \int_{\mathbb{R}^3} \cdot d\boldsymbol{\xi}. \quad (4)$$

For any given integer $M \geq 3$, we let

$$\mathbb{I}_M = \{\alpha \in \mathbb{N}^3, |\alpha| = \alpha_1 + \alpha_2 + \alpha_3 \leq M\}, \quad N = \#\mathbb{I}_M.$$

In virtue of the ordering of multi-indices (represented by the square brackets), we call the moment variable \mathbf{w} ‘‘induced’’ from \mathbb{I}_M with

$$\mathbf{w}[\alpha] \triangleq w_\alpha = w_\alpha(y).$$

The above notations are rigorously specified in Appendix A. Then M is called the moment order and the perturbation of the velocity distribution function in the Knudsen layer can be approximated by the Hermite series

$$f = f(y, \boldsymbol{\xi}) = \omega(\boldsymbol{\xi}) \sum_{\alpha \in \mathbb{I}_M} w_\alpha(y) \phi_\alpha(\boldsymbol{\xi}). \quad (5)$$

The formula (5) relates the moment variable with physical quantities in the Knudsen layer. For example, the density ρ , the temperature θ , the macro velocity $\mathbf{u} = (u_1, u_2, u_3)$, the stress tensor σ_{ij} , and the pressure p are defined as

$$\rho = \langle f \rangle, \quad u_i = \langle \xi_i f \rangle, \quad \theta = \left\langle \left(\frac{|\boldsymbol{\xi}|^2}{3} - 1 \right) f \right\rangle, \quad p = \rho + \theta, \quad \sigma_{ij} + p\delta_{ij} = \langle \xi_i \xi_j f \rangle. \quad (6)$$

The matrices $\mathbf{A}_2 \in \mathbb{R}^{N \times N}$ and $\mathbf{Q} \in \mathbb{R}^{N \times N}$ are induced (see Appendix A) from $\mathbb{I}_M \times \mathbb{I}_M$ with

$$\mathbf{A}_2[\alpha, \beta] = \langle \xi_2 \omega \phi_\alpha \phi_\beta \rangle = \sqrt{\alpha_2} \delta_{\beta, \alpha - e_2} + \sqrt{\alpha_2 + 1} \delta_{\beta, \alpha + e_2}, \quad (7)$$

$$\mathbf{Q}[\alpha, \beta] = \langle \omega \mathcal{L}(\phi_\beta) \phi_\alpha \rangle. \quad (8)$$

Here the operator \mathcal{L} is the linearized Boltzmann operator defined by

$$\mathcal{L}(\phi) = -\frac{1}{B_0} \omega^{-1} (\mathcal{Q}(\omega, \omega\phi) + \mathcal{Q}(\omega\phi, \omega)),$$

where B_0 is a constant representing the average collision frequency, and \mathcal{Q} is the Boltzmann collision operator defined as

$$\mathcal{Q}(g, h) = \frac{1}{2} \int_{\mathbb{R}^3} \int_{\mathbb{S}^2} (g'h'_* + g'_*h' - gh_* - g_*h) B(|\boldsymbol{\xi} - \boldsymbol{\xi}_*|, \boldsymbol{\Theta}) d\boldsymbol{\Theta} d\boldsymbol{\xi}_*.$$

Note that we write $g_* = g(t, \mathbf{x}, \boldsymbol{\xi}_*)$, $g' = g(t, \mathbf{x}, \boldsymbol{\xi}')$, $g'_* = g(t, \mathbf{x}, \boldsymbol{\xi}'_*)$, etc., for short. The pre-collisional velocities $\boldsymbol{\xi}'$ and $\boldsymbol{\xi}'_*$ are

$$\boldsymbol{\xi}' = \frac{\boldsymbol{\xi} + \boldsymbol{\xi}_*}{2} + \frac{|\boldsymbol{\xi} - \boldsymbol{\xi}_*|}{2} \boldsymbol{\Theta}, \quad \boldsymbol{\xi}'_* = \frac{\boldsymbol{\xi} + \boldsymbol{\xi}_*}{2} - \frac{|\boldsymbol{\xi} - \boldsymbol{\xi}_*|}{2} \boldsymbol{\Theta}, \quad \boldsymbol{\Theta} \in \mathbb{S}^2.$$

Let $\mathbf{g} = \boldsymbol{\xi} - \boldsymbol{\xi}_*$. The nonnegative function $B(|\mathbf{g}|, \boldsymbol{\Theta})$ is called the collision kernel.

In this paper, we consider the inverse-power-law (IPL) model. Now the collision kernel has the form [46]

$$B(|\mathbf{g}|, \boldsymbol{\Theta}) = |\mathbf{g}|^{\frac{\eta-5}{\eta-1}} W_0 \left| \frac{dW_0}{d\varphi} \right|,$$

where φ is the angle satisfying $\cos \varphi = \mathbf{g} \cdot \boldsymbol{\Theta} / |\mathbf{g}|$ and $\eta > 3$ is the index in the inverse-power potential. $3 < \eta < 5$ is called the soft potential and $\eta > 5$ is called the hard potential. When $\eta = 5$, it is the case of Maxwell molecules. When $\eta = +\infty$, the model can be regarded as the hard-sphere (HS) model. The dimensionless impact parameter W_0 is given by

$$\varphi = \pi - 2 \int_0^{W_1} \left(1 - W^2 - \frac{2}{\eta-1} \left(\frac{W}{W_0} \right)^{\eta-1} \right)^{-1/2} dW,$$

with W_1 a positive real number satisfying

$$1 - W_1^2 - \frac{2}{\eta-1} \left(\frac{W_1}{W_0} \right)^{\eta-1} = 0.$$

For the IPL intermolecular potentials defined above, it is classical [9] that $\mathcal{Q} \geq 0$.

2.2 General boundary conditions

Assume the boundary is fixed at the plane $\{\mathbf{x} \in \mathbb{R}^3, x_2 = 0\}$. In the kinetic theory, the general scattering BCs for the velocity distribution function $F(\boldsymbol{\xi})$ read as

$$\xi_2 F(\boldsymbol{\xi}) = \int_{\xi'_2 < 0} |\xi'_2| R(\boldsymbol{\xi}' \rightarrow \boldsymbol{\xi}) F(\boldsymbol{\xi}') d\boldsymbol{\xi}', \quad \xi_2 > 0. \quad (9)$$

The scattering kernel $R(\boldsymbol{\xi}' \rightarrow \boldsymbol{\xi})$ describes the probability that an incident molecule with the velocity $\boldsymbol{\xi}'$ is scattered to have the reflected velocity $\boldsymbol{\xi}$ lying in the range $d\boldsymbol{\xi}$. In principle, the scattering kernel is defined only for $\boldsymbol{\xi}$ and $\boldsymbol{\xi}'$ with $\xi_2 > 0$ as well as $\xi'_2 < 0$. The kernel $R(\boldsymbol{\xi}' \rightarrow \boldsymbol{\xi})$ must satisfy some general conditions [10] such as

- Nonnegativity. $R(\boldsymbol{\xi}' \rightarrow \boldsymbol{\xi}) \geq 0$, for all $\boldsymbol{\xi}, \boldsymbol{\xi}'$.
- Normalization.

$$\int_{\xi_2 > 0} R(\boldsymbol{\xi}' \rightarrow \boldsymbol{\xi}) d\boldsymbol{\xi} = 1, \quad \forall \boldsymbol{\xi}'. \quad (10)$$

- Detailed balance.

$$|\xi'_2| \omega(\boldsymbol{\xi}') R(\boldsymbol{\xi}' \rightarrow \boldsymbol{\xi}) = \xi_2 \omega(\boldsymbol{\xi}) R(-\boldsymbol{\xi} \rightarrow -\boldsymbol{\xi}'). \quad (11)$$

The linearized Maxwell diffuse-specular scattering kernel [32] reads as

$$R(\boldsymbol{\xi}' \rightarrow \boldsymbol{\xi}) = R_M(\boldsymbol{\xi}' \rightarrow \boldsymbol{\xi}) = \chi \frac{\xi_2}{2\pi} \exp\left(-\frac{|\boldsymbol{\xi}'|^2}{2}\right) + (1 - \chi)\delta(\boldsymbol{\xi}' - \boldsymbol{\xi}^*), \quad (12)$$

where $\chi \in [0, 1]$ is the tangential momentum accommodation coefficient (TMAC) and $\boldsymbol{\xi}^* = (\xi_1, -\xi_2, \xi_3)$. The linearized Cercignani-Lampis (CL) scattering kernel [10] reads as

$$\begin{aligned} R(\boldsymbol{\xi}' \rightarrow \boldsymbol{\xi}) &= R_{CL}(\boldsymbol{\xi}' \rightarrow \boldsymbol{\xi}) = \\ &= \frac{\xi_2}{2\pi\alpha_n\alpha_t(2-\alpha_t)} I_0\left(\frac{\sqrt{1-\alpha_n}}{\alpha_n}\xi_2\xi_2'\right) \exp\left(-\frac{\xi_2^2 + (1-\alpha_n)\xi_2'^2}{2\alpha_n} - \frac{|\boldsymbol{\xi}_t - (1-\alpha_t)\boldsymbol{\xi}_t'|^2}{2\alpha_t(2-\alpha_t)}\right), \end{aligned} \quad (13)$$

where $0 < \alpha_n \leq 1$ and $0 < \alpha_t < 2$ are two accommodation coefficients (ACs). Here $\boldsymbol{\xi}_t = (\xi_1, \xi_3)$ and the modified Bessel function

$$I_0(x) = \frac{1}{2\pi} \int_0^{2\pi} \exp(x \cos(\varphi)) d\varphi.$$

When $\alpha_n = \alpha_t = 1$, the CL BCs turn to the fully diffuse case, samely as $\chi = 1$ in the Maxwell BCs. As $\alpha_n \rightarrow 0$ and $\alpha_t \rightarrow 0$, the specular BCs are recovered. When $\alpha_n \rightarrow 0$ and $\alpha_t \rightarrow 2$, we have the bounce-back condition. The CL BCs are far from general [12] but simple and accurate enough to be used in practice.

We follow Grad's framework [16] to construct the BCs for moment equations (1) by testing the kinetic BCs (9) with even polynomials (about ξ_2). Choosing the Hermite polynomials ϕ_α with even α_2 as test functions gives

$$\int_{\xi_2 > 0} \xi_2 F(\boldsymbol{\xi}) \phi_\alpha(\boldsymbol{\xi}) d\boldsymbol{\xi} = \int_{\xi_2 > 0} \int_{\xi_2' < 0} |\xi_2'| R(\boldsymbol{\xi}' \rightarrow \boldsymbol{\xi}) F(\boldsymbol{\xi}') d\boldsymbol{\xi}' \phi_\alpha(\boldsymbol{\xi}) d\boldsymbol{\xi}. \quad (14)$$

We write the velocity distribution function as

$$F(\boldsymbol{\xi}) = f(0, \boldsymbol{\xi}) + \bar{F}(\boldsymbol{\xi}),$$

where f is the perturbation defined in (5) and $\bar{F}(\boldsymbol{\xi})$ is regarded as the given velocity distribution function of the bulk flow. Analogously as (5), we assume

$$\bar{F}(\boldsymbol{\xi}) = \omega(\boldsymbol{\xi}) \sum_{\alpha \in \mathbb{I}_M} \bar{w}_\alpha \phi_\alpha(\boldsymbol{\xi}).$$

Plugging (5) and the above formula into (14), denoting

$$K(\boldsymbol{\xi}' \rightarrow \boldsymbol{\xi}) = \frac{1}{\xi_2} R(\boldsymbol{\xi}' \rightarrow \boldsymbol{\xi}) \omega(\boldsymbol{\xi}'), \quad \xi_2 > 0, \xi_2' < 0,$$

we have the BCs for the moment variable \boldsymbol{w} :

$$\begin{aligned} &\sum_{|\beta| \leq M} (w_\beta(0) + \bar{w}_\beta) \int_{\xi_2 > 0} \xi_2 \omega(\boldsymbol{\xi}) \phi_\beta(\boldsymbol{\xi}) \phi_\alpha(\boldsymbol{\xi}) d\boldsymbol{\xi} \\ &= \sum_{|\beta| \leq M} (w_\beta(0) + \bar{w}_\beta) \int_{\xi_2 > 0} \int_{\xi_2' < 0} \xi_2 |\xi_2'| K(\boldsymbol{\xi}' \rightarrow \boldsymbol{\xi}) \phi_\beta(\boldsymbol{\xi}') \phi_\alpha(\boldsymbol{\xi}) d\boldsymbol{\xi}' d\boldsymbol{\xi}, \end{aligned} \quad (15)$$

where α_2 is even and \bar{w}_α are regarded as given by the bulk flow.

Remark 1. The detailed balance (11) of $R(\boldsymbol{\xi}' \rightarrow \boldsymbol{\xi})$ ensures the reciprocity of $K(\boldsymbol{\xi}' \rightarrow \boldsymbol{\xi})$, i.e.,

$$K(\boldsymbol{\xi}' \rightarrow \boldsymbol{\xi}) = K(-\boldsymbol{\xi} \rightarrow -\boldsymbol{\xi}').$$

For simplicity, we write the half-space integrals as

$$S(\boldsymbol{\alpha}, \boldsymbol{\beta}) = \int_{\xi_2 > 0} \xi_2 \omega(\boldsymbol{\xi}) \phi_{\boldsymbol{\beta}}(\boldsymbol{\xi}) \phi_{\boldsymbol{\alpha}}(\boldsymbol{\xi}) d\boldsymbol{\xi}. \quad (16)$$

In order to analyze, we make an even continuation such that $K(\boldsymbol{\xi}' \rightarrow \boldsymbol{\xi}) = K(-\boldsymbol{\xi}' \rightarrow \boldsymbol{\xi})$ for $\boldsymbol{\xi}' \in \mathbb{R}^3$. Then we define

$$R(\boldsymbol{\alpha}, \boldsymbol{\beta}) = \int_{\xi_2 > 0} \xi_2 \left(\int_{\mathbb{R}^3} K(\boldsymbol{\xi}' \rightarrow \boldsymbol{\xi}) \phi_{\boldsymbol{\beta}}(\boldsymbol{\xi}') d\boldsymbol{\xi}' \right) \phi_{\boldsymbol{\alpha}}(\boldsymbol{\xi}) d\boldsymbol{\xi}. \quad (17)$$

Since the whole space integral about odd functions are zero, we have $R(\boldsymbol{\alpha}, \boldsymbol{\beta}) = 0$ when β_2 is odd. If all the mentioned integrals exist and the Fubini theorem holds, we have

$$\begin{aligned} & \int_{\xi_2 > 0} \int_{\xi'_2 < 0} \xi_2 |\xi'_2| K(\boldsymbol{\xi}' \rightarrow \boldsymbol{\xi}) \phi_{\boldsymbol{\beta}}(\boldsymbol{\xi}') \phi_{\boldsymbol{\alpha}}(\boldsymbol{\xi}) d\boldsymbol{\xi}' d\boldsymbol{\xi} \\ &= \int_{\xi'_2 < 0} |\xi'_2| \left(\int_{\xi_2 > 0} \xi_2 K(\boldsymbol{\xi}' \rightarrow \boldsymbol{\xi}) \phi_{\boldsymbol{\alpha}}(\boldsymbol{\xi}) d\boldsymbol{\xi} \right) d\boldsymbol{\xi}' \phi_{\boldsymbol{\beta}}(\boldsymbol{\xi}') \\ &= \int_{\xi'_2 < 0} |\xi'_2| \sum_{\boldsymbol{\gamma} \in \mathbb{N}^3} \left(\int_{\mathbb{R}^3} \left(\int_{\xi_2 > 0} \xi_2 K(\boldsymbol{\xi}' \rightarrow \boldsymbol{\xi}) \phi_{\boldsymbol{\alpha}}(\boldsymbol{\xi}) d\boldsymbol{\xi} \right) \phi_{\boldsymbol{\gamma}}(\boldsymbol{\xi}') d\boldsymbol{\xi}' \right) \phi_{\boldsymbol{\beta}}(\boldsymbol{\xi}') \phi_{\boldsymbol{\gamma}}(\boldsymbol{\xi}') \omega(\boldsymbol{\xi}') d\boldsymbol{\xi}' \\ &= \sum_{\boldsymbol{\gamma} \in \mathbb{N}^3} R(\boldsymbol{\alpha}, \boldsymbol{\gamma}) \int_{\xi'_2 < 0} |\xi'_2| \phi_{\boldsymbol{\beta}}(\boldsymbol{\xi}') \phi_{\boldsymbol{\gamma}}(\boldsymbol{\xi}') \omega(\boldsymbol{\xi}') d\boldsymbol{\xi}' \\ &= \sum_{\boldsymbol{\gamma} \in \mathbb{N}^3} R(\boldsymbol{\alpha}, \boldsymbol{\gamma}) S(\boldsymbol{\gamma}, \boldsymbol{\beta}) (-1)^{\beta_2 + \gamma_2}. \end{aligned}$$

Meanwhile, the normalization property (10) gives $R(\mathbf{0}, \boldsymbol{\beta}) = \delta_{\boldsymbol{\beta}, \mathbf{0}}$.

Now we give the detailed choice of the test functions. We split the multi-indices into even and odd subsets, i.e.,

$$\mathbb{I}_{M,e} = \{\boldsymbol{\alpha} \in \mathbb{N}^3 : |\boldsymbol{\alpha}| \leq M, \alpha_2 \text{ even}\}, \quad \mathbb{I}_{M,o} = \{\boldsymbol{\alpha} \in \mathbb{N}^3 : |\boldsymbol{\alpha}| \leq M, \alpha_2 \text{ odd}\}.$$

Let $m = \#\mathbb{I}_{M,e}$ and $n = \#\mathbb{I}_{M,o}$. We immediately have $m + n = N$ with $m \geq n$. So as in Grad's framework, [16] a natural choice of the test functions is $\phi_{\boldsymbol{\alpha}}$ with $\boldsymbol{\alpha} \in \mathbb{I}_{M-1,e}$. The choice exactly gives $n = \#\mathbb{I}_{M-1,e}$ BCs. Let $\boldsymbol{w} = [\boldsymbol{w}_e^T, \boldsymbol{w}_o^T]^T$ and $\bar{\boldsymbol{w}} = [\bar{\boldsymbol{w}}_e^T, \bar{\boldsymbol{w}}_o^T]^T$. Here $\boldsymbol{w}_e \in \mathbb{R}^m$ and $\bar{\boldsymbol{w}}_e \in \mathbb{R}^m$ are induced (see Appendix A) from $\mathbb{I}_{M,e}$ and $\boldsymbol{w}_o \in \mathbb{R}^n, \bar{\boldsymbol{w}}_o \in \mathbb{R}^n$ are induced from $\mathbb{I}_{M,o}$. For any positive integers I and J , assume that the matrix $\boldsymbol{M}_{I,J}$ is induced from $\mathbb{I}_{I,e} \times \mathbb{I}_{J,o}$, and $\boldsymbol{S}_{I,J}, \boldsymbol{R}_{I,J}$ are induced from $\mathbb{I}_{I,e} \times \mathbb{I}_{J,e}$, with the entries

$$\boldsymbol{M}_{I,J}[\boldsymbol{\alpha}, \boldsymbol{\beta}] = 2S(\boldsymbol{\alpha}, \boldsymbol{\beta}), \quad \boldsymbol{S}_{I,J}[\boldsymbol{\alpha}, \boldsymbol{\beta}] = S(\boldsymbol{\alpha}, \boldsymbol{\beta}), \quad \boldsymbol{R}_{I,J}[\boldsymbol{\alpha}, \boldsymbol{\beta}] = R(\boldsymbol{\alpha}, \boldsymbol{\beta}). \quad (18)$$

Then from (15), the BCs of the moment equations (1) can write in the even-odd parity form

$$\begin{aligned} & (\boldsymbol{S}_{M-1,M} - \boldsymbol{R}_{M-1,J} \boldsymbol{S}_{J,M})(\boldsymbol{w}_e(0) + \bar{\boldsymbol{w}}_e) \\ & + \frac{1}{2}(\boldsymbol{M}_{M-1,M} + \boldsymbol{R}_{M-1,J} \boldsymbol{M}_{J,M})(\boldsymbol{w}_o(0) + \bar{\boldsymbol{w}}_o) = \mathbf{0}, \end{aligned} \quad (19)$$

where $\boldsymbol{M}_{M-1,M} \in \mathbb{R}^{n \times n}$, $\boldsymbol{S}_{M-1,M} \in \mathbb{R}^{n \times m}$, and J is any positive integer.

Remark 2. In general, the BCs in (19) is equivalent to the corresponding ones in (15) when $J = \infty$. But for the CL scattering kernel, we will show below (in Theorem 2) that

$$R(\boldsymbol{\alpha}, \boldsymbol{\beta}) = 0, \quad \text{when } \beta_2 > \alpha_2.$$

So $J = M - 1$ is enough in the CL case.

3 Solvability of the Layer Equations

To ensure the unique solvability of the layer equations (1):

$$\mathbf{A}_2 \frac{d\mathbf{w}}{dy} = -\mathbf{Q}\mathbf{w}, \quad \mathbf{w}(\infty) = \mathbf{0}, \quad y \in [0, +\infty),$$

the proper number of BCs at $y = 0$ relies on not only the eigenvalues of the boundary matrix, i.e., $-\mathbf{A}_2$ here, but also the null space structure of \mathbf{Q} . As shown in Ref.[16, 7], the $N \times N$ matrix \mathbf{A}_2 has n positive eigenvalues, n negative eigenvalues and $m - n$ zero eigenvalues. It's classical [9] that the linearized Boltzmann operator has a five-dimensional null space. Accordingly, we have [24] $\text{Null}(\mathbf{Q}) = \text{span}\{\varphi_0, \varphi_1, \varphi_2, \varphi_3, \varphi_4\}$, where φ_i are vectors induced from \mathbb{I}_M with the non-zero entries

$$\varphi_0[\mathbf{0}] = 1, \quad \varphi_i[\mathbf{e}_i] = 1, \quad 1 \leq i \leq 3, \quad \varphi_4[2\mathbf{e}_d] = \sqrt{3}/3, \quad 1 \leq d \leq 3.$$

From (6), we have $\varphi_0^T \mathbf{w} = \rho$, $\varphi_i^T \mathbf{w} = u_i$, $1 \leq i \leq 3$, and $\varphi_4^T \mathbf{w} = \frac{\sqrt{6}}{2}\theta$. Then Theorem 1 in Ref.[24] shows that the layer equations (1) need $n - 4$ BCs at $y = 0$ to determine a unique $\mathbf{w}(y)$.

The above result is different from the well-posed theory of the initial boundary value problem (IBVP), where n BCs are needed. [21] To agree with the IBVP, we also impose n BCs for the layer equations (1). Therefore, the given values $\bar{\mathbf{w}}_e$ and $\bar{\mathbf{w}}_o$ in the BCs (19) should not be arbitrary but satisfy 4 additional conditions. Theorem 2 in Ref.[24] shows that a special structure of the BCs would ensure the solvability, i.e.,

Theorem 1. *If we equip the layer equations (1) with the following n BCs at $y = 0$:*

$$\mathbf{M}_{M,M}^T (\mathbf{w}_e(0) + \bar{\mathbf{w}}_e) + \mathbf{H} (\mathbf{w}_o(0) + \bar{\mathbf{w}}_o) = \mathbf{0}, \quad (20)$$

where $\mathbf{M}_{M,M} \in \mathbb{R}^{m \times n}$ is defined in (18) and $\mathbf{H} \in \mathbb{R}^{n \times n}$ is any symmetric positive definite matrix, then there exists a unique solution of $\mathbf{w}(y)$ and $\varphi_i^T \bar{\mathbf{w}}, i = 0, 1, 3, 4$, when other components of $\bar{\mathbf{w}}$ are arbitrarily given. In particular, the solution would give $\varphi_2^T \mathbf{w}(y) = u_2(y) = 0$.

Unfortunately, (19) is not in the form of (20). For the Maxwell diffuse-specular case, (19) is shown unstable when $m > n$ for the non-homogeneous layer equations. [25] The reason lies in that the linear space determined by the BCs does not contain the null space of the boundary matrix. [31, 34] In Ref.[34, 24], the Maxwell BCs are modified to agree with the structure in (20). A basic tool in Ref.[24] is the following lemma:

Lemma 1. *For any positive integer I and J , the matrix $\mathbf{S}_{I,I}$ is symmetric positive definite. The matrix $\mathbf{M}_{I,J}$ is lower triangular. When $I \geq J$, the matrix $\mathbf{M}_{I,J}$ is of full column rank.*

To apply the solvability theorem 1 for general gas-surface scattering kernels, we follow Ref.[34]'s idea to modify (19) as minor as possible such that the modified BCs have the form as (20). We first let $J = M - 1$ in (19) and change all $\mathbf{S}_{M-1,M}$ to $\mathbf{S}_{M-1,M-1}$. This way discards the highest order moment variables when $m > n$. Then we try to inverse the coefficient matrix before $\mathbf{w}_e + \bar{\mathbf{w}}_e$ to meet the form in (20). However, due to the normalization property (10) of $R(\boldsymbol{\xi}' \rightarrow \boldsymbol{\xi})$, the corresponding coefficient matrix (i.e., $\mathbf{I} - \mathbf{R}_{M-1,M-1}$ in (21)) is irreversible. We should make a clever rank-one modification to ensure the invertibility (of $\mathbf{I} - \hat{\mathbf{R}}$ in (21)). In a word, the modified BCs read as

$$\begin{aligned} \mathbf{M}_{M,M}^T (\mathbf{w}_e(0) + \bar{\mathbf{w}}_e) + \mathbf{H} (\mathbf{w}_o(0) + \bar{\mathbf{w}}_o) &= \mathbf{0}, \\ \mathbf{H} &= \frac{1}{2} \mathbf{M}_{M-1,M}^T \left\{ \mathbf{S}_{M-1,M-1}^{-1} \left(\mathbf{I} - \hat{\mathbf{R}} \right)^{-1} \left(\mathbf{I} + \hat{\mathbf{R}} \right) \right\} \mathbf{M}_{M-1,M}, \\ \hat{\mathbf{R}} &= \mathbf{R}_{M-1,M-1} - \frac{\mathbf{S}_{M-1,M-1} \mathbf{e} \mathbf{e}^T}{\mathbf{e}^T \mathbf{S}_{M-1,M-1} \mathbf{e}} \in \mathbb{R}^{n \times n}, \end{aligned} \quad (21)$$

where \mathbf{I} is the n -th order identity matrix and $\mathbf{e} \in \mathbb{R}^n$ is a unit vector induced from $\mathbb{I}_{M-1,e}$ with $\mathbf{e}[\mathbf{0}] = 1$. We claim that the modified BCs (21) has the structure as (20):

Lemma 2. If $\hat{\mathbf{R}}$ satisfies $\rho(\hat{\mathbf{R}}) = k < 1$ and

$$\hat{\mathbf{R}}\mathbf{S}_{M-1,M-1} = \mathbf{S}_{M-1,M-1}\hat{\mathbf{R}}^T, \quad (22)$$

then the matrix \mathbf{H} defined in (21) is symmetric positive definite. Here $\rho(\hat{\mathbf{R}})$ is the spectral radius defined as the maximum modulus eigenvalues of $\hat{\mathbf{R}}$.

Proof. By Lemma 1, we have $\mathbf{S}_{M-1,M-1} > 0$. Since $\rho(\hat{\mathbf{R}}) < 1$, the matrix $\mathbf{I} - \hat{\mathbf{R}}$ is invertible. Let $\mathbf{X} = (\mathbf{I} - \hat{\mathbf{R}})^{-1}\mathbf{M}_{M-1,M} \in \mathbb{R}^{n \times n}$. Utilizing (22), we have

$$\mathbf{S}_{M-1,M-1}^{-1} - \hat{\mathbf{R}}^T \mathbf{S}_{M-1,M-1}^{-1} \hat{\mathbf{R}} = (\mathbf{I} - \hat{\mathbf{R}}^T) \mathbf{S}_{M-1,M-1}^{-1} (\mathbf{I} + \hat{\mathbf{R}}).$$

Noting that $(\mathbf{I} - \hat{\mathbf{R}})^{-1}(\mathbf{I} + \hat{\mathbf{R}}) = (\mathbf{I} + \hat{\mathbf{R}})(\mathbf{I} - \hat{\mathbf{R}})^{-1}$, from (21) we have

$$\mathbf{H} = \frac{1}{2} \mathbf{X}^T \left(\mathbf{S}_{M-1,M-1}^{-1} - \hat{\mathbf{R}}^T \mathbf{S}_{M-1,M-1}^{-1} \hat{\mathbf{R}} \right) \mathbf{X}.$$

Although $\hat{\mathbf{R}}$ may not be symmetric, the condition (22) gives

$$\mathbf{S}_{M-1,M-1}^{-1/2} \hat{\mathbf{R}} \mathbf{S}_{M-1,M-1}^{1/2} = \left(\mathbf{S}_{M-1,M-1}^{-1/2} \hat{\mathbf{R}} \mathbf{S}_{M-1,M-1}^{1/2} \right)^T.$$

Since similar matrices have the same eigenvalues, we have $\|\mathbf{S}_{M-1,M-1}^{-1/2} \hat{\mathbf{R}} \mathbf{S}_{M-1,M-1}^{1/2}\|_2 = k$. So for any $\mathbf{y} \in \mathbb{R}^n$, we have

$$\begin{aligned} & \mathbf{y}^T \left(\mathbf{S}_{M-1,M-1}^{-1} - \hat{\mathbf{R}}^T \mathbf{S}_{M-1,M-1}^{-1} \hat{\mathbf{R}} \right) \mathbf{y} \\ &= \mathbf{y}^T \mathbf{S}_{M-1,M-1}^{-1/2} \left(\mathbf{I} - \left(\mathbf{S}_{M-1,M-1}^{1/2} \hat{\mathbf{R}}^T \mathbf{S}_{M-1,M-1}^{-1} \hat{\mathbf{R}} \mathbf{S}_{M-1,M-1}^{1/2} \right) \right) \mathbf{S}_{M-1,M-1}^{-1/2} \mathbf{y} \\ &\geq \left(1 - \|\mathbf{S}_{M-1,M-1}^{1/2} \hat{\mathbf{R}} \mathbf{S}_{M-1,M-1}^{1/2}\|_2^2 \right) \mathbf{y}^T \mathbf{S}_{M-1,M-1}^{-1} \mathbf{y} \\ &\geq (1 - k^2) \mathbf{y}^T \mathbf{S}_{M-1,M-1}^{-1} \mathbf{y}. \end{aligned}$$

Thus, under the lemma's conditions, the matrix $\mathbf{S}_{M-1,M-1}^{-1} - \hat{\mathbf{R}}^T \mathbf{S}_{M-1,M-1}^{-1} \hat{\mathbf{R}}$ is symmetric positive definite. Combined with Lemma 1, the matrix \mathbf{H} in (21) is also symmetric positive definite. \square

Remark 3. The matrix $\hat{\mathbf{R}}$ in (21) is constructed from the belief that the solutions of (1) with (19) should be recovered from the solutions of (1) with the modified BCs (21) under some conditions. When $J = M - 1$ and $m = n$ (the condition $m = n$ is possible when $\alpha \in \mathbb{N}$ and M is odd), we have $\mathbf{M}_{M-1,M} = \mathbf{M}_{M,M}$ invertible and $\mathbf{S}_{M-1,M-1} = \mathbf{S}_{M-1,M}$. So the modified BCs (21) are equivalent to

$$(\mathbf{S}_{M-1,M} - \hat{\mathbf{R}}\mathbf{S}_{M-1,M})(\mathbf{w}_e + \bar{\mathbf{w}}_e) + \frac{1}{2}(\mathbf{M}_{M-1,M} + \hat{\mathbf{R}}\mathbf{M}_{M-1,M})(\mathbf{w}_o + \bar{\mathbf{w}}_o) = \mathbf{0}.$$

Since $\mathbf{M}_{M-1,M}$ is lower triangular, when $\mathbf{w}_o[\mathbf{e}_1] = \bar{\mathbf{w}}_o[\mathbf{e}_1] = 0$ and $\hat{\mathbf{R}}$ is defined as (21), we have

$$(\hat{\mathbf{R}} - \mathbf{R}_{M-1,M-1})\mathbf{M}_{M-1,M}(\mathbf{w}_o + \bar{\mathbf{w}}_o) = \mathbf{0}.$$

Compared with (19), we try to find $\rho^w \in \mathbb{R}$ such that

$$(\mathbf{S}_{M-1,M} - \hat{\mathbf{R}}\mathbf{S}_{M-1,M})(\mathbf{w}_e + \rho^w \mathbf{e}) = (\mathbf{S}_{M-1,M} - \mathbf{R}_{M-1,M-1}\mathbf{S}_{M-1,M})\mathbf{w}_e.$$

If the detailed balance condition (22) and the normalization condition $\mathbf{R}_{M-1,M-1}^T \mathbf{e} = \mathbf{e}$ hold, after some manipulation we find that $\hat{\mathbf{R}}^T \mathbf{e} = \mathbf{0}$ and

$$\rho^w = \mathbf{e}^T \mathbf{S}_{M-1,M} \mathbf{w}_e / \mathbf{e}^T \mathbf{S}_{M-1,M} \mathbf{e}.$$

Hence, the recovery is easy to obtain.

For general gas-surface scattering kernels, if the conditions in Lemma 2 hold, then Theorem 1 ensures the solvability of the layer equations (1) with the modified BCs (21). We can see that the condition (22) is naturally from the detailed balance property (11) of $R(\boldsymbol{\xi}' \rightarrow \boldsymbol{\xi})$. We do not try to check the condition $\rho(\hat{\mathbf{R}}) < 1$ for general BCs. But as will be shown below, the matrix $\hat{\mathbf{R}}$ is lower triangular for the CL scattering kernel. Hence, the spectral radius of $\hat{\mathbf{R}}$ in the CL case is easy to obtain (see Theorem 2 below).

4 The Cercignani-Lampis Scattering Kernel

For the CL scattering kernel, we will give the recursion formula to calculate the coefficient matrices in (21). The CL scattering kernel $K(\boldsymbol{\xi}' \rightarrow \boldsymbol{\xi})$ in (17) has the separability and can write as

$$K(\boldsymbol{\xi}' \rightarrow \boldsymbol{\xi}) = K_1(\xi_1, \xi'_1)K_2(\xi_2, \xi'_2)K_3(\xi_3, \xi'_3),$$

where for $i = 1$ and $i = 3$,

$$K_i(\xi_i, \xi'_i) = \frac{1}{\sqrt{2\pi\alpha_t(2-\alpha_t)}} \exp\left(-\frac{|\xi_i - (1-\alpha_t)\xi'_i|^2}{2\alpha_t(2-\alpha_t)}\right) \omega_0(\xi'_i), \quad (23)$$

and

$$K_2(\xi_2, \xi'_2) = \frac{1}{\sqrt{2\pi\alpha_n}} I_0\left(\frac{\sqrt{1-\alpha_n}}{\alpha_n} \xi_2 \xi'_2\right) \exp\left(-\frac{\xi_2^2 + \xi_2'^2}{2\alpha_n}\right). \quad (24)$$

The Hermite polynomials ϕ_α are isotropic and can write as

$$\phi_\alpha(\boldsymbol{\xi}) = \phi_{\alpha_1}(\xi_1)\phi_{\alpha_2}(\xi_2)\phi_{\alpha_3}(\xi_3), \quad \omega(\boldsymbol{\xi}) = \prod_{i=1}^3 \omega_0(\xi_i),$$

where we denote by $\phi_{\alpha_i} = \phi_{\alpha_i}(\xi_i) = \phi_{\alpha_i \mathbf{e}_i}(\boldsymbol{\xi})$ and $\omega_0(\xi_i) = (\sqrt{2\pi})^{-1} \exp(-\xi_i^2/2)$. The task is to calculate the integrals $S(\boldsymbol{\alpha}, \boldsymbol{\beta})$ and $R(\boldsymbol{\alpha}, \boldsymbol{\beta})$ in (16) and (17). Due to the separability, these integrals are products of two-dimensional integrals. Here $R(\boldsymbol{\alpha}, \boldsymbol{\beta})$ is a combination of the modified Bessel function, Hermite polynomials, exponentials, and powers.

According to the orthogonality of Hermite polynomials, we have

$$S(\boldsymbol{\alpha}, \boldsymbol{\beta}) = \delta_{\alpha_1, \beta_1} \delta_{\alpha_3, \beta_3} S_0(\alpha_2, \beta_2), \quad (25)$$

where for $\alpha_2, \beta_2 \in \mathbb{N}$, we define the half-space integral

$$S_0(\alpha_2, \beta_2) = \int_0^{+\infty} \xi_2 \phi_{\alpha_2} \phi_{\beta_2} \omega_0(\xi_2) d\xi_2. \quad (26)$$

A direct calculation gives (see Appendix B)

Lemma 3. *When α_2 is even and β_2 is odd, we have*

$$S_0(\alpha_2, \beta_2) = \frac{1}{2} \left(\sqrt{\alpha_2} \delta_{\beta_2, \alpha_2-1} + \sqrt{\alpha_2+1} \delta_{\beta_2, \alpha_2+1} \right).$$

When α_2 and β_2 are both even, we have

$$S_0(\alpha_2, \beta_2) = \frac{1}{\sqrt{2\pi}} \frac{\alpha_2 + \beta_2 + 1}{1 - (\alpha_2 - \beta_2)^2} z^{\alpha_2} z^{\beta_2},$$

where $z_0 = 1$ and $z_{n+1} = -\sqrt{n}z_{n-1}/\sqrt{n+1}$.

For the CL BCs, the integral $R(\boldsymbol{\alpha}, \boldsymbol{\beta})$ involves the half-space integrals about $K_i(\xi_i, \xi'_i)$. When $i = 1$ and $i = 3$, the corresponding integrals are explicitly given in virtue of the symmetry of $K_i(\xi_i, \xi'_i)$ (see Appendix C).

Lemma 4. For $\alpha_1, \beta_1 \in \mathbb{N}$, the integral

$$T(\alpha_1, \beta_1) = \int_{\mathbb{R}^2} \phi_{\beta_1}(\xi'_1) \phi_{\alpha_1}(\xi_1) K_1(\xi_1, \xi'_1) d\xi'_1 d\xi_1 \quad (27)$$

has the explicit expression

$$T(\alpha_1, \beta_1) = \delta_{\alpha_1, \beta_1} (1 - \alpha_t)^{\alpha_1}.$$

On the other hand, we do not find a ready-made formula to calculate the integral about $K_2(\xi_2, \xi'_2)$. For even α_2 , we denote by

$$N(\alpha_2; \xi'_2) = \exp\left(\frac{\xi_2'^2}{2\alpha_n}\right) \int_{\xi_2 > 0} \xi_2 K_2(\xi_2, \xi'_2) \phi_{\alpha_2}(\xi_2) d\xi_2 \quad (28)$$

and claim that (proof in Appendix D)

Lemma 5. $N(\alpha_2; \xi'_2)$ can be represented as

$$N(\alpha_2; \xi'_2) = \omega_0(\xi'_2) \exp\left(\frac{\xi_2'^2}{2\alpha_n}\right) \sum_{\beta_2=0}^{\alpha_2} r_{\alpha_2, \beta_2} \phi_{\beta_2}(\xi'_2),$$

where r_{α_2, β_2} are constant coefficients which are zero when β_2 is odd. The recursion relation of r_{α_2, β_2} is given in Appendix D. In particular, we have

$$r_{\alpha_2, \alpha_2} = (1 - \alpha_n)^{\alpha_2}.$$

Due to the orthogonality of Hermite polynomials, we immediately have

$$R(\boldsymbol{\alpha}, \boldsymbol{\beta}) = \delta_{\alpha_1, \beta_1} \delta_{\alpha_3, \beta_3} (1 - \alpha_t)^{\alpha_1 + \alpha_3} r_{\alpha_2, \beta_2}, \quad (29)$$

where $r_{\alpha_2, \beta_2} = 0$ for $\beta_2 > \alpha_2$. So we can conclude that

Theorem 2. Suppose $M \geq 3$. For the CL scattering kernel, the matrix $\hat{\mathbf{R}}$ in (21) is lower triangular. The spectral radius is

$$\rho(\hat{\mathbf{R}}) = \max(|1 - \alpha_t|, 1 - \alpha_n).$$

Hence, when $0 < \alpha_t < 2$ and $0 < \alpha_n \leq 1$, the conditions in Lemma 2 hold for the CL BCs.

Proof. Recalling that $\hat{\mathbf{R}}$ is a rank-one modification of $\mathbf{R}_{M-1, M-1}$ (see (21)) and the elements of $\mathbf{R}_{M-1, M-1}$ are $R(\boldsymbol{\alpha}, \boldsymbol{\beta})$ with α_2 and β_2 even. When α_2 and β_2 are both even, by definition in Appendix A, $\boldsymbol{\beta}$ is ordered after $\boldsymbol{\alpha}$ if and only if $\alpha_i \neq \beta_i$ for any $i = 1, 3$, or $\alpha_i = \beta_i$ for $i = 1, 3$, but $\beta_2 > \alpha_2$. In both cases, from (29), we have $R(\boldsymbol{\alpha}, \boldsymbol{\beta}) = 0$. Hence, $\mathbf{R}_{M-1, M-1}$ is lower triangular and so is $\hat{\mathbf{R}}$.

The eigenvalues of the lower triangular matrix are their diagonal elements. By Lemma 5 and (29), we have

$$R(\boldsymbol{\alpha}, \boldsymbol{\alpha}) = (1 - \alpha_t)^{\alpha_1 + \alpha_3} (1 - \alpha_n)^{\alpha_2}.$$

So $\mathbf{R}_{M-1, M-1}$ must have the eigenvalue one, corresponding to $R(\mathbf{0}, \mathbf{0})$. But the rank-one modification removes the eigenvalue one, which gives

$$\hat{\mathbf{R}}[\boldsymbol{\alpha}, \boldsymbol{\alpha}] = (1 - \alpha_t)^{\alpha_1 + \alpha_3} (1 - \alpha_n)^{\alpha_2} - \delta_{\boldsymbol{\alpha}, \mathbf{0}}.$$

So when $0 < \alpha_t < 2$ and $0 < \alpha_n \leq 1$, we have $\rho(\hat{\mathbf{R}}) < 1$. By definition, the condition (22) in Lemma 2 also holds. \square

Combined with the above theorem, Lemma 2 and Theorem 1, we obtain the solvability of the CL BCs (21).

Example 1 (Fully diffuse BCs). Now $\alpha_t = \alpha_n = 1$ and the conditions in Lemma 2 hold. From (29) and the recursion relation of r_{α_2, β_2} in Appendix D, we find that $\hat{\mathbf{R}} = \mathbf{0}$.

Example 2 (Specular BCs). This is a limiting case when $\alpha_t \rightarrow 0$ and $\alpha_n \rightarrow 0$. Now according to Theorem 2, the conditions in Lemma 2 do not hold. However, the direct calculation from (29) shows that $\mathbf{R}_{M-1, M-1}$ should be an identity matrix. So the original BCs (19) give

$$\mathbf{M}_{M-1, M}(\mathbf{w}_o + \bar{\mathbf{w}}_o) = \mathbf{0} \quad \Rightarrow \quad \mathbf{w}_o + \bar{\mathbf{w}}_o = \mathbf{0}.$$

We can easily check the solvability in this special case.

In conclusion, for the CL scattering kernel, all the integrals in (21) are determined by explicit recursion relations. The procedure avoids numerical integration and the evaluation of the modified Bessel function. The total computation cost of $S(\boldsymbol{\alpha}, \boldsymbol{\beta})$ and $R(\boldsymbol{\alpha}, \boldsymbol{\beta})$ is $O(M^2)$ operations. For more general BCs, we may have to utilize numerical integration to calculate the half-space integrals, where Gauss-Hermite quadratures or other ununiform quadratures should be cleverly used.

5 Slip and Jump Coefficients

5.1 Mathematical formulation

In the spirit of the Chapman-Enskog expansion, [9] the half-space problems have the same governing equations (1) but different driven terms $\bar{\mathbf{w}}$ in the BCs (21).

In Kramers' problem, [23] the tangential flow in the Knudsen layer is assumed to be driven by the normal velocity gradient at infinity. So Kramers' problem is defined as the layer equations (1) with the BCs, denoting by $\mathbf{B} = [\mathbf{M}_{M, M}^T, \mathbf{H}] \in \mathbb{R}^{n \times N}$ in (21),

$$\mathbf{B}(\mathbf{w} - (\partial U / \partial x_2)_\infty \mathbf{z}_k + \bar{\mathbf{w}}_0) = \mathbf{0}. \quad (30)$$

Here $(\partial U / \partial x_2)_\infty$ is a given constant and $\bar{\mathbf{w}}_0 \in \text{Null}(\mathbf{Q})$ with $\boldsymbol{\varphi}_2^T \bar{\mathbf{w}}_0 = \bar{\mathbf{w}}_0[\mathbf{e}_2] = 0$. The given driven term $\mathbf{z}_k \in \mathbb{R}^N$ belongs to $\text{Null}(\mathbf{Q})^\perp$ and is derived from the Chapman-Enskog expansion, satisfying

$$\mathbf{Q} \mathbf{z}_k = \mathbf{r}_{12},$$

where \mathbf{Q} is the coefficient matrix in (1), corresponding to the linearized Boltzmann operator, and $\mathbf{r}_{12} \in \mathbb{R}^N$ is induced from \mathbb{I}_M with $\mathbf{r}_{12}[\mathbf{e}_1 + \mathbf{e}_2] = 1$. Due to Theorem 1, we can solve a linear relation between $\boldsymbol{\varphi}_1^T \bar{\mathbf{w}}_0$ and $(\partial U / \partial x_2)_\infty$. Denote by $\bar{u} = \boldsymbol{\varphi}_1^T \bar{\mathbf{w}}_0$, then we define the viscous-slip coefficient ζ_0 as

$$\zeta_0 = \frac{\bar{u}}{\sqrt{2} \gamma_1 (\partial U / \partial x_2)_\infty}, \quad \gamma_1 = \mathbf{r}_{12}^T \mathbf{z}_k. \quad (31)$$

Here γ_1 is a normalized viscosity coefficient and ζ_0 is the ratio of the slip length to the mean free path. In the Knudsen layer, the normalized velocity profile $u_d(y)$ is defined by

$$u_d(y) = -\frac{u_1(y)}{\sqrt{2} \gamma_1 (\partial U / \partial x_2)_\infty},$$

where $u_1(y) = \mathbf{w}[\mathbf{e}_1]$.

Analogously, the thermal creep problem considers the tangential flow driven by the tangential gradient of the temperature. According to the Chapman-Enskog procedure, we define the thermal creep problem as the layer equations (1) with the BCs

$$\mathbf{B}(\mathbf{w} - (\partial T / \partial x_1)_\infty \mathbf{z}_c + \bar{\mathbf{w}}_0) = \mathbf{0}, \quad (32)$$

where $(\partial T / \partial x_1)_\infty$ is a given constant and $\mathbf{z}_c \in \text{Null}(\mathbf{Q})^\perp$ is given as the solution of

$$\mathbf{Q} \mathbf{z} = \mathbf{s}_1.$$

Here \mathbf{s}_1 is induced from \mathbb{I}_M with $\mathbf{s}_1[3\mathbf{e}_1] = \sqrt{3/2}$, $\mathbf{s}_1[\mathbf{e}_1 + 2\mathbf{e}_d] = \sqrt{1/2}$, $d \neq 1$. Similarly we define the thermal-slip coefficient as

$$\zeta_1 = \frac{\bar{u}}{2\gamma_2(\partial T/\partial x_1)_\infty}, \quad \gamma_2 = \frac{2}{5}\mathbf{s}_1^T \mathbf{z}_c, \quad (33)$$

and the normalized velocity in the Knudsen layer is

$$u_d(y) = -\frac{u_1(y)}{2\gamma_2(\partial T/\partial x_1)_\infty}.$$

Here γ_2 can be seen as the normalized thermal conductivity coefficient.

The temperature jump problem [47] is a thermal version of Kramers' problem. The problem considers the heat transfer in the Knudsen layer driven by the normal temperature gradient of the bulk flow. This gives the layer equations (1) with the BCs

$$\mathbf{B}(\mathbf{w} - (\partial T/\partial x_2)_\infty \mathbf{z}_t + \bar{\mathbf{w}}_0) = \mathbf{0}, \quad (34)$$

where $(\partial T/\partial x_2)_\infty$ is a given constant and $\mathbf{z}_t \in \text{Null}(\mathbf{Q})^\perp$ is given as the solution of

$$\mathbf{Q}\mathbf{z} = \mathbf{s}_2.$$

The non-zero entries of \mathbf{s}_2 are $\mathbf{s}_2[3\mathbf{e}_2] = \sqrt{3/2}$, $\mathbf{s}_2[\mathbf{e}_2 + 2\mathbf{e}_d] = \sqrt{1/2}$, $d \neq 2$. Now we let $\bar{\mathbf{w}}[2\mathbf{e}_i] = \bar{\theta}/\sqrt{2}$ and the temperature-jump coefficient is analogously defined as

$$\zeta_2 = \frac{\bar{\theta}}{\sqrt{2}\gamma_2(\partial T/\partial x_2)_\infty}. \quad (35)$$

The relation (6) gives $\sum_{i=1}^3 \mathbf{w}[2\mathbf{e}_i] = \frac{3\sqrt{2}}{2}\theta(y)$ and we define the normalized temperature in the Knudsen layer as

$$\theta_d(y) = -\frac{\theta(y)}{\sqrt{2}\gamma_2(\partial T/\partial x_2)_\infty}.$$

The above half-space problems can be solved universally by the method proposed in our early work. [24] The method is analytical in principle and concluded as follows:

1. Solve the generalized eigenvalue problem of $(\mathbf{A}_2, \mathbf{Q})$ to obtain general solutions to (1).
2. Plug the necessary conditions such that the general solution of (1) satisfies $\mathbf{w}(\infty) = \mathbf{0}$ into the BCs (21). Solve the obtained linear system to get $\mathbf{w}(0)$.
3. Obtain $\mathbf{w}(y)$ according to the expressions of the general solution to (1).

The calculation of the matrices \mathbf{Q} and \mathbf{B} would be another challenge because, by definition, their elements are high-dimensional integrals (eight-dimensional for \mathbf{Q} and six-dimensional for \mathbf{B}). We use the ready-made \mathbf{Q} calculated by numerical integration in Ref.[46] for IPL potentials. The matrix \mathbf{B} for the CL scattering kernel is calculated by the recursion relations in Sec.4. As will be shown below, the analytical procedure provides us with not only an accurate result of \mathbf{B} , but also explicit expressions of the slip and jump coefficients in terms of the ACs.

To reduce the computation cost, we consider the BGK-type approximation of \mathbf{Q} . [46] Namely, for a given constant L , $\mathbf{Q}[\boldsymbol{\alpha}, \boldsymbol{\beta}]$ are exactly calculated from the linearized Boltzmann operator when $|\boldsymbol{\alpha}|, |\boldsymbol{\beta}| \leq L$, while the remaining part of \mathbf{Q} is approximated by a diagonal matrix. Combined with the sparsity pattern of \mathbf{A}_2 , \mathbf{B} and $\bar{\mathbf{w}}$, we can extract $O(ML^2)$ effective equations from the total $O(M^3)$ equations in (1). The reduced procedure has been described in detail in Ref.[24], which makes the layer equations (1) computable when M is large. In this paper, we let $L = 20$ and M may be several hundred.

5.2 Numerical results

As far as we know, very little data on slip and jump coefficients are available for the IPL intermolecular potentials and CL gas-surface interaction. The subsection validates the efficiency and accuracy of the moment model in the above cases for different moment order M .

We first consider the hard-sphere (HS) case where $\eta = \infty$ in the IPL model. In Fig.1, we let $\alpha_t = \alpha_n = 1$ and calculate the coefficients $\zeta_i, i = 0, 1, 2$, for M ranging from 5 to 84. The label “N” represents the results given by the modified BCs (21), while “G” represents the results given by the Grad BCs (19). We see that all the coefficients will converge when M becomes larger. The results approach their limit from both ends according to the parity of M for the modified BCs, while only from below in the case of the Grad BCs.

Note that the instability of (19), if exists, is about the non-homogeneous term in the layer equations, [25] which would not affect the solvability of homogeneous equations. In comparison, we can see that the boundary stabilization does not affect the accuracy too much.

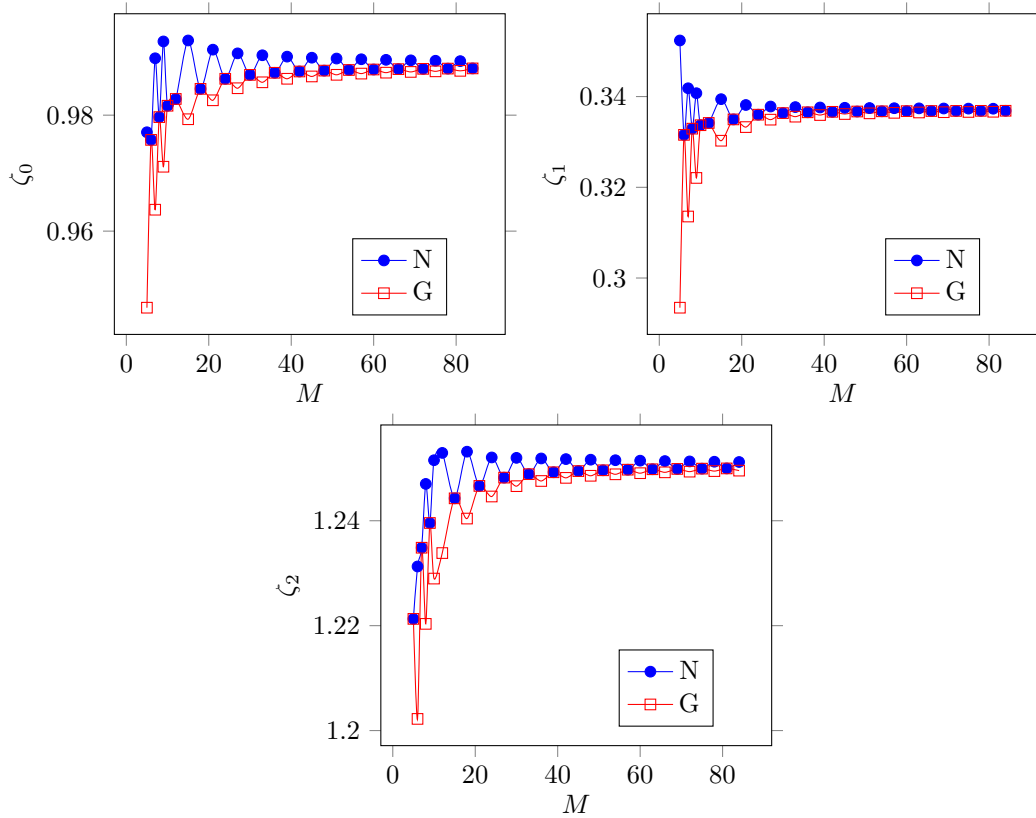


Figure 1: Convergence tests of the coefficients ζ_i in the HS model, with $\alpha_t = \alpha_n = 1$.

In Fig.2, we choose α_t and α_n as their corner values, i.e., α_t close to 0 or 2 and α_n close to 0. The convergence of the viscous-slip coefficient ζ_0 is also observed. This shows the stability of our algorithm at the limiting cases. Similar results are observed for the thermal-slip coefficient ζ_1 and temperature-jump coefficient ζ_2 (not exhibited here).

We then study the influence of the moment order. For $M = 4, 10, 50$, we calculate the slip coefficients $\zeta_i, i = 0, 1$, for $\alpha_n \in [0, 1]$, $\alpha_t \in [0.25, 2]$. For $M = 5, 11, 51$, we calculate the temperature-jump coefficient ζ_2 for $\alpha_n \in [0, 1]$, $\alpha_t \in [0.25, 1]$. Note that when α_n is fixed, α_t and $2 - \alpha_t$ would give the same jump coefficient ζ_2 . So we cut the range of α_t in half in the temperature jump problem. The results are individually shown in Tab.1, Tab.2, and Tab.3. Because the parity of M is the same in one table, we expect to see the convergence from one side in the same table.

In Tab.1, the highly accurate viscous-slip coefficients calculated from the LBE [41] are included.

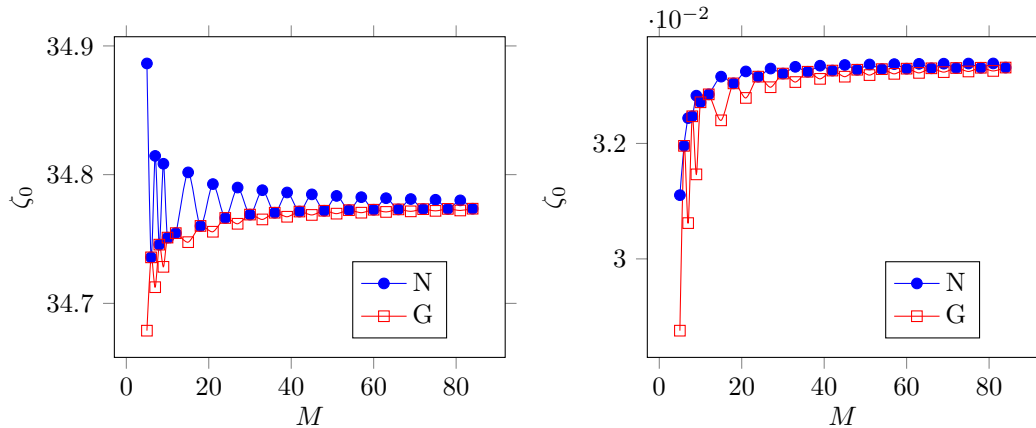


Figure 2: Convergence tests of the coefficient ζ_0 in the HS model. Left: $\alpha_t = 0.05, \alpha_n = 0.05$. Right: $\alpha_t = 1.95, \alpha_n = 0.05$.

We see that when $\alpha_t < 1$, the slip coefficient ζ_0 slightly decreases when α_n increases. The trend reverses when $\alpha_t > 1$. When $\alpha_t = 1$, the slip coefficient ζ_0 does not vary with α_n . When $\alpha_t < 1$, the moment model with $M = 4$ has already given accurate ζ_0 , whose relative errors, compared to the results of $M = 50$ or Ref.[41], are less than 3%. When α_t and α_n are both large, the lowest order moment model with $M = 4$ is not accurate, where the relative errors are larger than 10%. But the moment model with mild order such as $M = 10$ performs well, obtaining the relative errors less than 5% even in some limiting cases. The BGK-type approximation of \mathbf{Q} may be another reason that the obtained ζ_0 when $M = 50$ slightly deviates from the results of Ref.[41], i.e., with the relative errors less than 0.1% in most cases.

In Tab.2, we list thermal-slip coefficients for the CL BCs and compare our results with the LBE's. [36, 45] We find that the relative errors of the moment model with $M = 50$ and Ref.[36] are about 0.1% in most cases. Compared to the viscous-slip coefficient ζ_0 , the variation of ζ_1 is smaller when α_t changes. When α_t is fixed and α_n increases, the thermal-slip coefficient ζ_1 decreases when $\alpha_t < 1$, remaining unchanged when $\alpha_t = 1$, and increases when $\alpha_t > 1$. In the thermal creep problem, the moment model with $M = 4$ is enough to provide an accurate ζ_1 with the relative errors less than 3% compared with Ref.[36].

In Tab.3, we compare our temperature-jump coefficients with the results of the LBE. [36] We find that the temperature-jump coefficient ζ_2 decreases when α_n and $\alpha_t \leq 1$ turn larger. Analogously, the moment model with $M = 5$ seems enough to provide a relatively accurate temperature-jump coefficient.

For the sake of brevity, we do not show the results of other IPL potentials here, although the comparison has been accomplished for the Maxwell molecules ($\eta = 5$) and some other available data in Ref.[41, 45]. In a word, all the results support that a mild moment model with $M \approx 10$ can capture slip and jump coefficients well even in some limiting cases.

We compare the wall clock time used for moment models with different M . Our code is not optimized and implemented by MATLAB R2019, running on the laptop with i7-8550U CPU @ 1.80GHz. In Fig.3, the label “time A” contains the cost to generate \mathbf{B} in the BCs, solving the generalized eigenvalue problem of $(\mathbf{A}_2, \mathbf{Q})$ and the linear algebraic system, but does not include the generation of \mathbf{Q} . That’s to say, \mathbf{Q} is calculated beforehand and read from the file. In reality, when the model is fixed, the eigenvalue problem only needs to solve once. So we also consider the “time B”, which does not contain the cost to solve the generalized eigenvalue problem compared with the “time A”.

In Fig.3, we repeatedly calculate the coefficients for 100 times and take the average wall time. We find that the main cost comes from solving the generalized eigenvalue problem. The “time B” for $M \leq 32$ is less than 1ms. When $M = 64$ (not shown in the figure), for the viscous-slip coefficient ζ_0 , the “time A” is about 3.57s and the “time B” is about 0.42s. Combined with the previous

Table 1: Viscous-slip coefficient ζ_0 for the Cercignani-Lampis BCs in the HS model

α_t	M	$\alpha_n = 0$	$\alpha_n = 0.25$	$\alpha_n = 0.5$	$\alpha_n = 0.75$	$\alpha_n = 1$
0.25	4	6.33938	6.32513	6.31093	6.29677	6.28265
	10	6.37510	6.35349	6.33403	6.31645	6.30045
	50	6.39435	6.36519	6.34284	6.32364	6.30659
	Ref.[41]		6.365427	6.343336	6.324267	6.307321
0.5	4	2.77490	2.76541	2.75593	2.74648	2.73704
	10	2.80361	2.78951	2.77674	2.76513	2.75449
	50	2.81737	2.79906	2.78456	2.77193	2.76060
	Ref.[41]		2.799516	2.785158	2.772602	2.761338
0.75	4	1.57406	1.56933	1.56459	1.55987	1.55515
	10	1.59673	1.58982	1.58354	1.57779	1.57249
	50	1.60617	1.59751	1.59046	1.58423	1.57859
	Ref.[41]		1.598122	1.591127	1.584932	1.579323
1.0	4	0.964293	0.964293	0.964293	0.964293	0.964293
	10	0.981622	0.981622	0.981622	0.981622	0.981622
	50	0.987722	0.987722	0.987722	0.987722	0.987722
	Ref.[41]		0.988451	0.988451	0.988451	0.988451
1.25	4	0.590920	0.595624	0.600333	0.605047	0.609765
	10	0.603435	0.610081	0.616170	0.621810	0.627080
	50	0.607019	0.614835	0.621529	0.627585	0.633179
	Ref.[41]		0.615670	0.622315	0.628343	0.633906
1.5	4	0.335520	0.344908	0.354315	0.363740	0.373184
	10	0.343598	0.356670	0.368685	0.379875	0.390396
	50	0.345383	0.360302	0.373369	0.385333	0.396489
	Ref.[41]		0.361248	0.374217	0.386121	0.397213
1.75	4	0.147115	0.161201	0.175327	0.189493	0.203700
	10	0.151032	0.170357	0.188173	0.204852	0.220632
	50	0.151646	0.173077	0.192246	0.210003	0.226713
	Ref.[41]		0.174178	0.193187	0.210840	0.227456
2.0	4	0	0.0188546	0.0377750	0.0567615	0.0758145
	10	0	0.0254564	0.0489856	0.0711298	0.0922059
	50	0	0.0274630	0.0525196	0.0759943	0.0982846
	Ref.[41]		0.028851	0.053665	0.076984	0.099153

results that a mild order moment model performs well, we conclude that the moment model is very efficient and accurate in capturing slip and jump coefficients.

5.3 Explicit expressions

In this subsection, we focus on the CL scattering kernel and IPL potentials. The moment model is analytical in the sense that i) the formal solution of the layer equations (1) is available and ii) the Hermite expansion of CL BCs is explicitly given. Therefore, when M is small, we can write explicit expressions about slip and jump coefficients. These formulae are functions of the ACs, i.e., α_t and α_n in the CL kernel. The coefficients in the formulae are different for different IPL intermolecular potentials.

First we consider the viscous-slip coefficient ζ_0 . When $M = 2$, the moment model gives the formula

$$\zeta_0 = \frac{2 - \alpha_t \sqrt{\pi}}{\alpha_t} \frac{\sqrt{\pi}}{2} \quad (36)$$

for all the IPL potentials. The formula (36) is independent of the intermolecular potential and the accommodation coefficient α_n , agreeing with the literature. [29, 50] Compared with Tab.1, (36)

Table 2: Thermal-slip coefficient ζ_1 for the Cercignani-Lampis BCs in the HS model

α_t	M	$\alpha_n = 0$	$\alpha_n = 0.25$	$\alpha_n = 0.5$	$\alpha_n = 0.75$	$\alpha_n = 1$
0.25	4	0.262909	0.281742	0.300515	0.319229	0.337884
	10	0.268408	0.288734	0.308258	0.327055	0.345200
	50	0.270170	0.290853	0.310756	0.329846	0.348224
0.5	Ref.[36]	0.26960	0.29049	0.31041	0.32950	0.34787
	4	0.281290	0.293648	0.305982	0.318290	0.330573
	10	0.287068	0.300106	0.312749	0.325029	0.336978
0.75	50	0.289701	0.302666	0.315457	0.327896	0.339998
	Ref.[36]	0.28905	0.30221	0.31503	0.32748	0.33958
	4	0.303436	0.309567	0.315691	0.321809	0.327921
1.0	10	0.309606	0.315927	0.322109	0.328162	0.334095
	50	0.312635	0.318802	0.325009	0.331123	0.337129
	Ref.[36]	0.31206	0.31834	0.32456	0.33068	0.33668
1.25	4	0.327544	0.327544	0.327544	0.327544	0.327544
	10	0.333690	0.333690	0.333690	0.333690	0.333690
	50	0.336727	0.336727	0.336727	0.336727	0.336727
1.5	Ref.[36]	0.33628	0.33628	0.33628	0.33628	0.33628
	4	0.351523	0.345443	0.339357	0.333265	0.327167
	10	0.357081	0.351070	0.345103	0.339177	0.333287
1.75	50	0.359766	0.354113	0.348222	0.342278	0.336326
	Ref.[36]	0.35944	0.35369	0.34778	0.34183	0.33588
	4	0.372951	0.360884	0.348794	0.336680	0.324542
2.0	10	0.377351	0.365636	0.353923	0.342203	0.330476
	50	0.379360	0.368544	0.357081	0.345375	0.333538
	Ref.[36]	0.37915	0.36813	0.35663	0.34491	0.33306
2.25	4	0.389169	0.371334	0.353448	0.335511	0.317523
	10	0.392014	0.374964	0.357779	0.340452	0.322989
	50	0.393091	0.377644	0.360983	0.343752	0.326151
2.5	Ref.[36]	0.39299	0.37723	0.36049	0.34323	0.32562
	4	0.397561	0.374363	0.351085	0.327725	0.304283
	10	0.398938	0.377003	0.354691	0.332010	0.308984
3.0	50	0.398936	0.379474	0.358082	0.335650	0.312491
	Ref.[36]	0.39894	0.37904	0.35751	0.33502	0.31183

would have a relatively large deviation above 10% in the HS model. To alleviate this deviation, Ref.[29, 22, 50] modify the formula as

$$\zeta_0 = \frac{2 - \alpha_t}{\alpha_t} \frac{\sqrt{\pi}}{2} (1 + 0.1366\alpha_t). \quad (37)$$

While in Ref.[26, 41], the formula reads as

$$\zeta_0 = \frac{a}{\alpha_t} - b\alpha_t - c, \quad (38)$$

where a, b , and c are fitting coefficients relying on the intermolecular potential and α_n . It's shown [41] that the above fitting formula can predict the LBE solutions well.

In comparison, the moment model with $M = 4$ gives a new explicit expression of ζ_0 . We omit the tedious process of the calculation here. The expression is very concise when we define some auxiliary parameters as

$$m_1 = \frac{2 - \alpha_t}{\alpha_t}, \quad m_2 = -1 + \frac{2}{\alpha_t(\alpha_t^2 - 3\alpha_t + 3)}, \quad m_3 = -1 + \frac{2}{\alpha_n + \alpha_t - \alpha_n\alpha_t}. \quad (39)$$

Table 3: Temperature-jump coefficient ζ_2 for the Cercignani-Lampis BCs in the HS model

α_t	M	$\alpha_n = 0$	$\alpha_n = 0.25$	$\alpha_n = 0.5$	$\alpha_n = 0.75$	$\alpha_n = 1$
0.25	5	9.99768	5.67986	3.73807	2.63537	1.92775
	11	10.1069	5.71826	3.76224	2.65729	1.95137
	51	10.1558	5.73315	3.77200	2.66686	1.96228
	Ref.[36]	10.151	5.7318	3.7707	2.6655	1.9609
0.5	5	5.76656	3.80951	2.69240	1.97267	1.47398
	11	5.86585	3.85425	2.71941	1.99401	1.49444
	51	5.90485	3.87043	2.72920	2.00205	1.50267
	Ref.[36]	5.9030	3.8696	2.7282	2.0010	1.5015
0.75	5	4.57861	3.16218	2.28852	1.69885	1.27783
	11	4.67225	3.20886	2.31758	1.72129	1.29831
	51	4.70607	3.22518	2.32781	1.72934	1.30606
	Ref.[36]	4.7049	3.2245	2.3270	1.7284	1.3050
1.0	5	4.28115	2.98966	2.17682	1.62125	1.22129
	11	4.37295	3.03675	2.20650	1.64413	1.24193
	51	4.40516	3.05304	2.21688	1.65225	1.24962
	Ref.[36]	4.4041	3.0524	2.2161	1.6514	1.2486

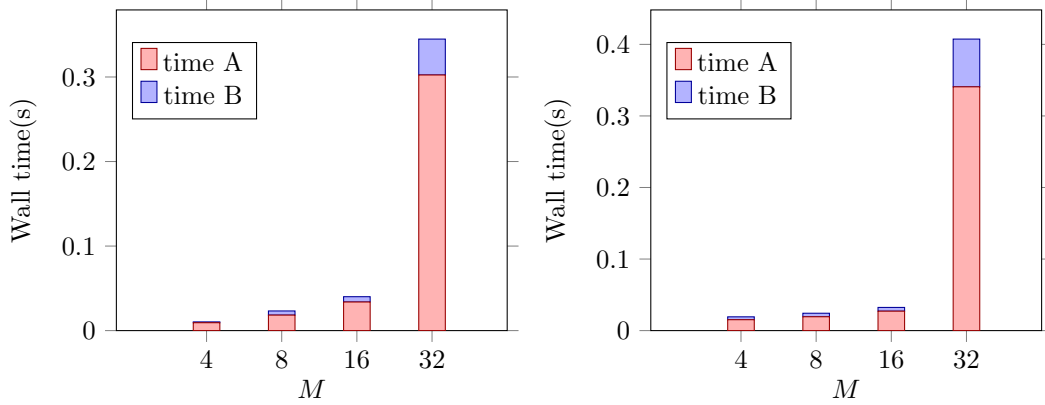


Figure 3: The wall time to calculate the slip/jump coefficients for different M in the HS model ($\alpha_n = \alpha_t = 1$). Left: the viscous-slip coefficient ζ_0 . Right: the temperature-jump coefficient ζ_2 .

The viscous-slip coefficient reads as

$$\zeta_0 = \frac{\sqrt{\pi}}{2} m_1 + \frac{d_1 m_2 + d_2 m_3 + d_3 m_2 m_3}{c_1 m_2 + c_2 m_3 + c_3 m_2 m_3 + c_4}, \quad (40)$$

where c_i and d_i are constants determined by the intermolecular potential. Tab.4 shows their values in some special cases. Note that there exists a freedom about these coefficients, so we may as well assume $c_4 = 1$. Compared to the formulae (36) and (38), the formula (40) has stronger nonlinearity about α_n and α_t . The accuracy of (40) in the HS model is shown in Tab.1, where the relative errors are less than 3% when $\alpha_t < 1$.

The formula (40) successfully explains two phenomena observed in numeric. I). A linear correction should be added to improve the accuracy of (36) as in (38) and (37). Fig.4 exhibits the dependence of $\zeta_0 - \sqrt{\pi} m_1 / 2$ about α_t when $M = 30$ and α_n is fixed. We can see that the relation is almost linear. In Ref.[50], the correction (37) for the CL case is heuristically given without rigorous derivation. Here, from Tab.4, we may approximately let $c_i = 1$, $d_1 = 0$ and $d_2 = d_3$ in

Table 4: Coefficients in (40) for the IPL models

η	c_1	c_2	c_3	c_4	d_1	d_2	d_3
∞ (HS)	0.9302	0.9861	0.9135	1	0.006073	0.1506	0.1423
5 (Maxwell molecules)	0.9346	0.9868	0.9203	1	0	0.2216	0.2071
10 (Hard potential)	0.9318	0.9856	0.9156	1	0.001965	0.1795	0.1673
3.1 (Soft potential)	0.9363	0.9874	0.9230	1	0.005607	0.3026	0.2921

(40), which gives

$$\zeta_0 = \frac{\sqrt{\pi}}{2} m_1 + d_2 \frac{m_3}{1+m_3} = \frac{\sqrt{\pi}}{2} m_1 + \frac{d_2}{2} (-(1-\alpha_n)\alpha_t + 2 - \alpha_n).$$

So the prediction of (40) agrees with Fig.4 qualitatively.

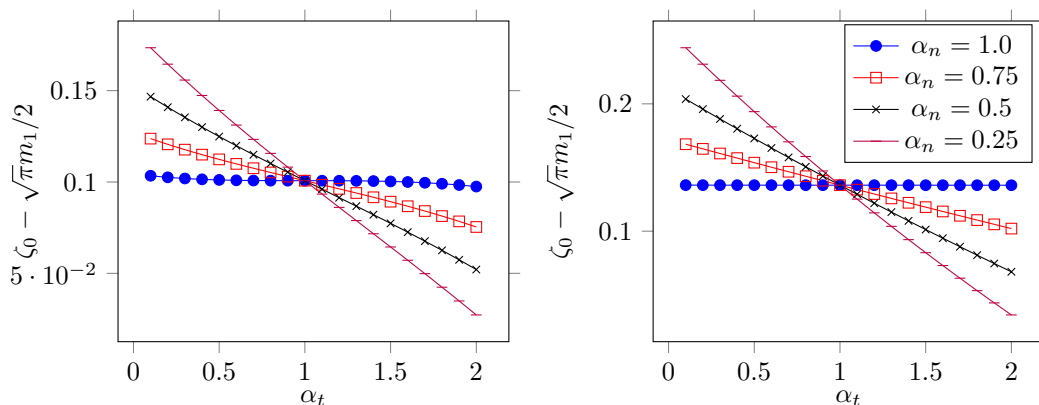


Figure 4: The dependence of $\zeta_0 - \sqrt{\pi}m_1/2$ about α_t . Left: HS model. Right: Maxwell molecules.

The formula (40) also predicts that II). when the first term $\sqrt{\pi}m_1/2$ dominates, the viscous-slip coefficient is insensitive to the intermolecular potentials. However, when α_t is close to 2, i.e., in the backward scattering case, the latter term in (40) will dominate. According to the values of d_2 and d_3 in Tab.4, we know that now the IPL model with $\eta = 3.1$ may have a viscous-slip coefficient twice as large as the HS model. In Tab.5, we compare the viscous-slip coefficient ζ_0 for different IPL potentials when $\alpha_t = 0.25, 0.5, 1.75, 2$, $\alpha_n \in [0.25, 1]$ and $M = 50$. We can see that the prediction of (40) agrees with our numerical results. The phenomena are also reported in the numerical results of Ref.[41].

Then we consider the thermal-slip coefficient ζ_1 . In Fig.5, we plot the relation of ζ_1 about α_t when $M = 30$ and α_n is fixed. We can see that ζ_1 is nonlinear about α_t and its trends on α_t differ according to the intermolecular potential. For example when $\alpha_n = 1$ and α_t increases, ζ_1 decreases in the HS model but increases in the soft potential case where $\eta = 3.1$. This phenomenon is also reported in Ref.[45].

The trends are different from the Maxwell diffuse-specular case, where ζ_1 is linear about χ when the other conditions are fixed. Here χ is the accommodation coefficient in the Maxwell accommodation BCs. For the Maxwell model, if the scaled thermal-slip coefficient is defined as

$$\sigma_T = \frac{5}{2} \sqrt{\frac{2}{\pi}} \frac{\gamma_2}{\gamma_1} \zeta_1,$$

then Maxwell gives the first approximation in history as

$$\sigma_T = \frac{3}{4},$$

Table 5: Viscous-slip coefficient ζ_0 for the Cercignani-Lampis BCs and IPL models ($M = 50$)

α_t	η	$\alpha_n = 0.25$	$\alpha_n = 0.5$	$\alpha_n = 0.75$	$\alpha_n = 1$
0.25	∞	6.36519	6.34284	6.32364	6.30659
	10	6.39080	6.36387	6.34040	6.31926
	5	6.42968	6.39653	6.36717	6.34037
	3.1	6.51376	6.46837	6.42748	6.38965
0.5	∞	2.79906	2.78456	2.77193	2.76060
	10	2.82086	2.80350	2.78811	2.77408
	5	2.85360	2.83237	2.81319	2.79545
	3.1	2.92349	2.89474	2.86824	2.84328
1.75	∞	0.173077	0.192246	0.210003	0.226713
	10	0.177461	0.199731	0.221007	0.241554
	5	0.185033	0.211481	0.237526	0.263340
	3.1	0.203235	0.237705	0.272854	0.308798
2	∞	0.0274630	0.0525196	0.0759943	0.0982846
	10	0.0303310	0.0592114	0.0871847	0.114498
	5	0.0343861	0.0684421	0.102506	0.136708
	3.1	0.0426832	0.0867627	0.132487	0.179964

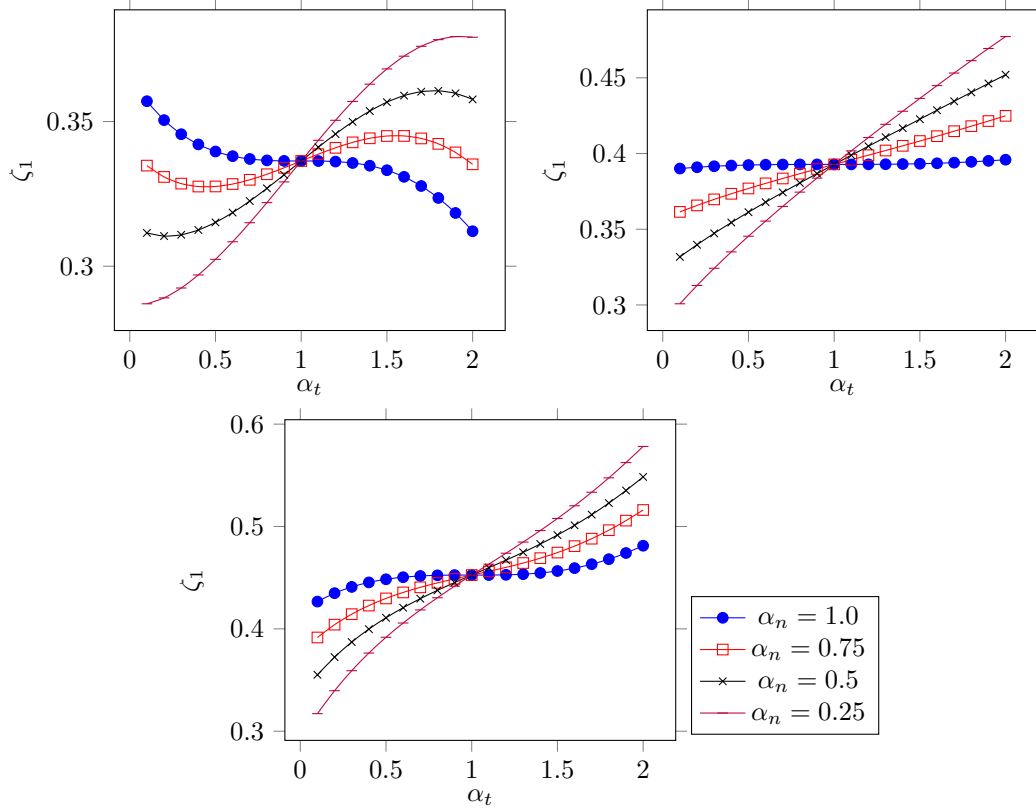


Figure 5: The dependence of ζ_1 about α_t . Left: HS model. Right: Maxwell molecules. Bottom: $\eta = 3.1$.

and Loyalka (cf. Ref.[28] and refs therein) modified it as

$$\sigma_T = \frac{3}{4} \left(1 + \frac{1}{2} \chi \right).$$

For the CL scattering kernel, the explicit formula for the thermal-slip coefficient is relatively rare. A formula derived from the variational method for the HS model is given by Ref.[33]. For the moment model with $M = 4$, we can derive the analytical expression of ζ_1 as

$$\zeta_1 = \frac{1}{4} + \frac{d_1 m_2 + d_2 m_3 + d_3}{c_1 m_2 + c_2 m_3 + c_3 m_2 m_3 + c_4}, \quad (41)$$

where m_2 and m_3 are the same as in (39). The constant coefficients c_i , d_i are determined by intermolecular potentials, given in Tab.6 for some special cases. Here we let $c_4 = 1$ again.

Table 6: Coefficients in (41) for the IPL models

η	c_1	c_2	c_3	c_4	d_1	d_2	d_3
∞ (HS)	0.9302	0.9861	0.9135	1	0.1892	-0.03975	0.1476
5 (Maxwell molecules)	0.9346	0.9868	0.9203	1	0.2336	0.01564	0.2500
10 (Hard potential)	0.9318	0.9856	0.9156	1	0.2085	-0.01632	0.1918
3.1 (Soft potential)	0.9363	0.9874	0.9230	1	0.2751	0.07147	0.3484

Compared with Ref.[33], the formula (41) is much simpler in form and suitable for all IPL potentials. As shown in Tab.2, the formula would give accurate thermal-slip coefficients with the relative errors less than 3% in the HS case. The formula (41) can also illustrate the phenomenon mentioned in the discussion of Fig.5. When $\alpha_n = 1$, we have $m_3 = 1$, which results in

$$\zeta_1 = \frac{1}{4} + \frac{d_1 m_2 + d_2 + d_3}{(c_1 + c_3)m_2 + c_2 + c_4}.$$

Apparently, if $d_1 > 0$ and $c_1 + c_3 > 0$, the above ζ_1 is an increasing function about m_2 when

$$\frac{d_2 + d_3}{d_1} < \frac{c_2 + c_4}{c_1 + c_3}.$$

According to Tab.6, we can check that it is the case of the HS model and the hard potential with $\eta = 10$. While for the Maxwell molecules and the soft potential with $\eta = 3.1$, the opposite inequality holds, and ζ_1 is a decreasing function about m_2 . Since m_2 is a decreasing function about α_t , when $\alpha_n = 1$, we have ζ_1 decreasing about α_t in the HS and $\eta = 10$ case, while increasing for the Maxwell molecules and $\eta = 3.1$ case. Unlike (40), there seems no dominant term in (41) and the dependence of ζ_1 on different IPL potentials is relatively complicated. Thermal-slip coefficients for different IPL potentials with $M = 50$ are shown in Tab.7.

Finally we focus on the temperature-jump coefficient ζ_2 . For the Maxwell diffuse-specular BCs, ζ_2 has explicit formulae like (38), i.e., a linear combination of $(2 - \chi)/\chi$, χ and 1. Corresponding formulae are given by Maxwell, [32] Welander, [47] and Loyalka. [30] There is less work about expressions of ζ_2 with the IPL intermolecular potentials and CL BCs.

When $M = 3$, we derive the analytical expression of ζ_2 from the moment model. In this case, ζ_2 is independent of the intermolecular potential and reads as

$$\zeta_2 = \frac{\frac{\sqrt{15}}{5} \left(\frac{9}{4} n_1 + n_2 \right) + \frac{5\sqrt{2}}{8} \sqrt{2\pi} n_1 n_2}{n_1 + n_2 + \sqrt{\frac{30}{2\pi}}}, \quad (42)$$

where

$$n_1 = \frac{2 - \alpha_n}{\alpha_n}, \quad n_2 = -1 + \frac{2}{\alpha_t(2 - \alpha_t)}. \quad (43)$$

The formula (42) is similar as the expressions in Ref.[39, 50]. It shows that ζ_2 would increase when α_n and α_t decrease. This coincides with the numerical results in Fig.6, where the dependence of ζ_2 on α_n and α_t is exhibited for the HS model when $M = 31$.

Table 7: Thermal-slip coefficient ζ_1 for the Cercignani-Lampis BCs and IPL models ($M = 50$)

α_t	η	$\alpha_n = 0.25$	$\alpha_n = 0.5$	$\alpha_n = 0.75$	$\alpha_n = 1$
0.25	∞	0.290853	0.310756	0.329846	0.348224
	10	0.302713	0.324813	0.346144	0.366798
	5	0.318814	0.343789	0.368016	0.391574
	3.1	0.349837	0.380177	0.409672	0.438373
0.5	∞	0.302666	0.315457	0.327896	0.339998
	10	0.321031	0.335170	0.349038	0.362633
	5	0.345619	0.361500	0.377187	0.392660
	3.1	0.391936	0.411003	0.429919	0.448637
1.75	∞	0.377644	0.360983	0.343752	0.326151
	10	0.412165	0.394188	0.375274	0.355639
	5	0.457493	0.437730	0.416661	0.394473
	3.1	0.540527	0.517270	0.492286	0.465637
2	∞	0.379474	0.358082	0.335650	0.312491
	10	0.422007	0.399075	0.374592	0.348866
	5	0.477440	0.452313	0.425143	0.396153
	3.1	0.578318	0.548573	0.516248	0.481319

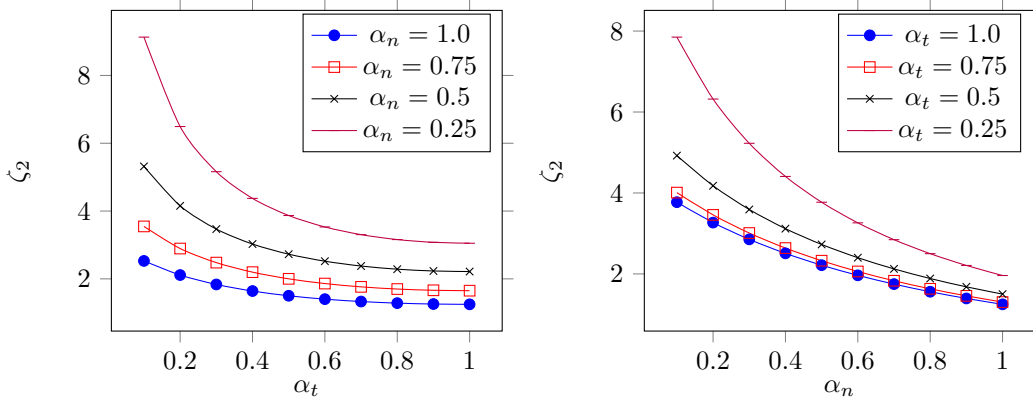


Figure 6: The dependence of ζ_2 in the HS model.

Tab.8 shows that the temperature-jump coefficient ζ_2 is insensitive to the IPL potentials. To improve the accuracy of (42), a possible way is to write the expression of ζ_2 when $M = 5$. However, the expression is too complicated to explicitly write down. An alternative method is to assume

$$\zeta_2 = \frac{d_1 n_1 + d_2 n_2 + d_3 n_1 n_2}{c_1 n_1 + c_2 n_2 + 1},$$

where c_i and d_i are fitting coefficients to be determined by intermolecular potentials.

The data fitting is also promising to improve the accuracy of (40) and (41). From this point of view, the analytical solutions to the moment model are instructive and help us find the critical parameters that affect slip and jump coefficients, i.e., m_i and n_i in (39) and (43). It may deserve a detailed discussion somewhere else about these fitting formulae compared with the experimental and MD data. The issue should be future work and beyond the scope of this paper.

6 Conclusions

Our main intention was to develop the moment method of arbitrary order for describing rarefied gas effects due to the general gas-surface interaction. Utilizing the Hermite expansion, we derived the layer equations with general boundary conditions in the frame of the moment method.

Table 8: Temperature-jump coefficient ζ_2 for different IPL models ($M = 51$)

α_t	η	$\alpha_n = 0$	$\alpha_n = 0.25$	$\alpha_n = 0.5$	$\alpha_n = 0.75$	$\alpha_n = 1$
0.25	∞	10.1558	5.73315	3.77200	2.66686	1.96228
	10	10.2440	5.78167	3.80694	2.69542	1.98856
	5	10.3696	5.85382	3.85960	2.73847	2.02783
	3.1	10.6213	6.00574	3.97211	2.83055	2.11117
0.5	∞	5.90485	3.87043	2.72920	2.00205	1.50267
	10	5.98305	3.91934	2.76441	2.03034	1.52837
	5	6.09432	3.99076	2.81680	2.07283	1.56697
	3.1	6.31497	4.13759	2.92688	2.16318	1.64920
0.75	∞	4.70607	3.22518	2.32781	1.72934	1.30606
	10	4.77847	3.27307	2.36293	1.75777	1.33201
	5	4.88165	3.34261	2.41483	1.80028	1.37094
	3.1	5.08564	3.48431	2.52300	1.89021	1.45378
1.0	∞	4.40516	3.05304	2.21688	1.65225	1.24962
	10	4.47565	3.10043	2.25189	1.68071	1.27568
	5	4.57622	3.16918	2.30354	1.72322	1.31477
	3.1	4.77494	3.30897	2.41098	1.81303	1.39792

These moment systems are proved solvable after a simple boundary stabilization. In particular, we discussed the Cercignani-Lampis scattering kernel and gave a recursion formula to calculate its Hermite expansion. This procedure avoids numerical integration and helps us find explicit expressions for slip and jump coefficients in terms of the accommodation coefficients.

Based on the moment model, we analyzed and evaluated viscous-slip, thermal-slip, and temperature-jump coefficients for the inverse-power-law intermolecular potentials and Cercignani-Lampis boundary conditions. As shown in numerical tests, our moment model can capture slip and jump coefficients accurately and efficiently with mild moments. For low-order moment models, explicit expressions of slip and jump coefficients about the accommodation coefficients were derived. These formulae are nonlinear, accurate, and concise in form, which successfully explain some reported effects of the accommodation coefficients and intermolecular potentials.

A Orders of multi-indices

Definition 1. We define the ordering \preceq on \mathbb{N}^D as follows. For $\boldsymbol{\alpha}, \boldsymbol{\beta} \in \mathbb{N}^D$,

1. If α_2 is even and β_2 is odd, then $\boldsymbol{\alpha} \preceq \boldsymbol{\beta}$.
2. If α_2 and β_2 have the same parity, but $|\boldsymbol{\alpha}| < |\boldsymbol{\beta}|$, then $\boldsymbol{\alpha} \preceq \boldsymbol{\beta}$.
3. If α_2 and β_2 have the same parity and $|\boldsymbol{\alpha}| = |\boldsymbol{\beta}|$, but there exists a smallest $1 \leq i \leq D$ such that $\alpha_i \neq \beta_i$, then $\boldsymbol{\alpha} \preceq \boldsymbol{\beta}$ if and only if $\alpha_i \geq \beta_i$.

As usual, $\boldsymbol{\alpha} < \boldsymbol{\beta}$ means $\boldsymbol{\alpha} \preceq \boldsymbol{\beta}$ and $\boldsymbol{\alpha} \neq \boldsymbol{\beta}$. In the above definition, a special feature is that the indices with an even second component are always ordered before the odd ones, e.g., the index $(a_1, 0, a_3)$ is ordered before $(b_1, 1, b_3)$ for any a_1, a_3, b_1 and b_3 . Except for that point, the multi-indices are first sorted by the multi-index norm and then by the anti-lexicographic order.

If \mathbb{I} is a subset of \mathbb{N}^D , then the ordering of \mathbb{I} is naturally defined as the restriction of \preceq to \mathbb{I} . If $\mathbb{I} \subset \mathbb{N}^D$ is finite with $\#\mathbb{I}$ elements, then \mathbb{I} is isomorphic to $\{1, 2, \dots, \#\mathbb{I}\}$. In this paper, we define the default isomorphism $\mathcal{N} : \mathbb{I} \rightarrow \{1, 2, \dots, \#\mathbb{I}\}$ by the ordering \preceq , i.e., $\mathcal{N}(\boldsymbol{\alpha}) \leq \mathcal{N}(\boldsymbol{\beta})$ if and only if $\boldsymbol{\alpha} \preceq \boldsymbol{\beta}$.

Here, if a vector \boldsymbol{w} is called induced from \mathbb{I} , we mean that the length of \boldsymbol{w} is $\#\mathbb{I}$ and we use $\boldsymbol{w}[\boldsymbol{\alpha}]$ to represent its $\mathcal{N}(\boldsymbol{\alpha})$ -th element where $\boldsymbol{\alpha} \in \mathbb{I}$. Analogously, if a matrix \boldsymbol{A} is called induced from $\mathbb{I}_1 \times \mathbb{I}_2$, then the size of \boldsymbol{A} is $(\#\mathbb{I}_1) \times (\#\mathbb{I}_2)$. For $\boldsymbol{\alpha} \in \mathbb{I}_1$ and $\boldsymbol{\beta} \in \mathbb{I}_2$, we use $\boldsymbol{A}[\boldsymbol{\alpha}, \boldsymbol{\beta}]$ to represent

its entry in the $\mathcal{N}_1(\boldsymbol{\alpha})$ -th row and $\mathcal{N}_2(\boldsymbol{\beta})$ -th column, where $\mathcal{N}_i, i = 1, 2$, are default isomorphic functions for \mathbb{I}_i .

B Calculation of $S_0(\alpha_2, \beta_2)$

From (26) and the recursion relation (3), we have

$$\begin{aligned} S_0(\alpha_2, \beta_2) &= \int_0^{+\infty} (\sqrt{\alpha_2} \phi_{\alpha_2-1} + \sqrt{\alpha_2+1} \phi_{\alpha_2+1}) \phi_{\beta_2} \omega_0(\xi_2) d\xi_2 \\ &= \sqrt{\alpha_2} I(\alpha_2-1, \beta_2) + \sqrt{\alpha_2+1} I(\alpha_2+1, \beta_2), \end{aligned} \quad (44)$$

where we define

$$I(\alpha_2, \beta_2) = \int_0^{+\infty} \phi_{\alpha_2} \phi_{\beta_2} \omega_0(\xi_2) d\xi_2.$$

According to integration by parts, noting that

$$\frac{d}{d\xi_2} (\omega_0(\xi_2) \phi_{\beta_2}) = -\sqrt{\beta_2+1} \omega_0(\xi_2) \phi_{\beta_2+1}, \quad \frac{d}{d\xi_2} \phi_{\alpha_2+1} = \sqrt{\alpha_2+1} \phi_{\alpha_2}, \quad (45)$$

we have

$$I(\alpha_2+1, \beta_2+1) = (\phi_{\alpha_2+1}(0) \phi_{\beta_2}(0) \omega_0(0) + \sqrt{\alpha_2+1} I(\alpha_2, \beta_2)) / \sqrt{\beta_2+1}. \quad (46)$$

The symmetry gives $I(\alpha_2, \beta_2) = I(\beta_2, \alpha_2)$. So we also have

$$I(\alpha_2+1, \beta_2+1) = (\phi_{\beta_2+1}(0) \phi_{\alpha_2}(0) \omega_0(0) + \sqrt{\beta_2+1} I(\alpha_2, \beta_2)) / \sqrt{\alpha_2+1}. \quad (47)$$

When $\alpha_2 \neq \beta_2$, we can equal (46) and (47) to obtain the explicit expression of $I(\alpha_2, \beta_2)$. For simplicity, we denote by $z_n = \phi_n(0)$. Then the recursion relation (3) gives

$$z_{n+1} = -\sqrt{n} z_{n-1} / \sqrt{n+1}$$

with $z_0 = 1$ and $z_1 = 0$. We also have $\omega_0(0) = (\sqrt{2\pi})^{-1}$. When $\alpha_2 = \beta_2$, noting that $z_n = 0$ when n is odd, we have $I(\alpha_2+1, \alpha_2+1) = I(\alpha_2, \alpha_2)$ with $I(0, 0) = 1/2$. From (44), we can finally write the expressions of $S_0(\alpha_2, \beta_2)$.

C Calculation of $T(\alpha_1, \beta_1)$

Assume the Fubini theorem holds such that we can exchange the integration order. We will calculate $T(\alpha_1, \beta_1)$ by induction. Let $\alpha_1 = 0$, then the orthogonality of Hermite polynomials gives

$$T(0, \beta_1) = \int_{\mathbb{R}} \phi_{\beta_1}(\xi'_1) \omega_0(\xi'_1) d\xi'_1 = \delta_{\beta_1, 0}.$$

Integrate by parts with (45) and use the recursion relation (3), then we have

$$\begin{aligned} Y_{\alpha_1} &\triangleq \int_{\mathbb{R}} \phi_{\alpha_1}(\xi_1) \exp\left(-\frac{|\xi_1 - (1-\alpha_t)\xi'_1|^2}{2\alpha_t(2-\alpha_t)}\right) d\xi_1 \\ &= \frac{1}{\sqrt{\alpha_1+1}} \int_{\mathbb{R}} \frac{\xi_1 - (1-\alpha_t)\xi'_1}{\alpha_t(2-\alpha_t)} \phi_{\alpha_1+1}(\xi_1) \exp\left(-\frac{|\xi_1 - (1-\alpha_t)\xi'_1|^2}{2\alpha_t(2-\alpha_t)}\right) d\xi_1 \\ &= \frac{1}{\sqrt{\alpha_1+1}} \int_{\mathbb{R}} \frac{-(1-\alpha_t)\xi'_1 \phi_{\alpha_1+1} + \sqrt{\alpha_1+1} \phi_{\alpha_1} + \sqrt{\alpha_1+2} \phi_{\alpha_1+2}}{\alpha_t(2-\alpha_t)} \exp\left(-\frac{|\xi_1 - (1-\alpha_t)\xi'_1|^2}{2\alpha_t(2-\alpha_t)}\right) d\xi_1 \end{aligned}$$

Collecting the terms, we have

$$\sqrt{\alpha_1}Y_{\alpha_1} = -(1 - \alpha_t)^2\sqrt{\alpha_1 - 1}Y_{\alpha_1 - 2} + (1 - \alpha_t)\xi_1'Y_{\alpha_1 - 1}, \quad \alpha_1 \geq 2, \quad (48)$$

with $Y_0 = 1$ and $Y_1 = (1 - \alpha_t)\xi_1'$. Using the recursion relation (3) to get rid of ξ_1' in (48) and recalling the definition of $T(\alpha_1, \beta_1)$, we have the recursion formula

$$\begin{aligned} T(\alpha_1, \beta_1) &= -(1 - \alpha_t)^2 \frac{\alpha_1 - 1}{\alpha_1} T(\alpha_1 - 2, \beta_1) \\ &\quad + (1 - \alpha_t) \frac{\sqrt{\beta_1}T(\alpha_1 - 1, \beta_1 - 1) + \sqrt{\beta_1 + 1}T(\alpha_1 - 1, \beta_1 + 1)}{\sqrt{\alpha_1}}. \end{aligned} \quad (49)$$

Here we let $T(-1, \beta_1) = 0$ and get

$$T(1, \beta_1) = \int_{\mathbb{R}} \phi_{\beta_1}(\xi_1') \omega_0(\xi_1') Y_1 d\xi_1' = (1 - \alpha_t) \delta_{\beta_1, 1}.$$

By induction, we can see that $T(\alpha_1, \beta_1) = 0$ when $\beta_1 > \alpha_1$.

However, by definition, we have the symmetry

$$T(\alpha_1, \beta_1) = T(\beta_1, \alpha_1).$$

So $T(\alpha_1, \beta_1) = 0$ when $\alpha_1 > \beta_1$, too. Thus, the recursion relation (49) becomes

$$T(\alpha_1, \alpha_1) = (1 - \alpha_t)T(\alpha_1 - 1, \alpha_1 - 1).$$

We finally have $T(\alpha_1, \beta_1) = \delta_{\alpha_1, \beta_1} (1 - \alpha_t)^{\alpha_1}$.

D Proof of Lemma 5

Firstly, we introduce some preliminaries. The series expansion of the zeroth order modified Bessel function (8.447 in Ref.[17]) is

$$I_0 \left(\frac{\sqrt{1 - \alpha_n}}{\alpha_n} \xi_2 \xi_2' \right) = \sum_{k=0}^{\infty} \frac{(1 - \alpha_n)^k}{(2\alpha_n)^{2k}} \frac{1}{(k!)^2} \xi_2^{2k} \xi_2'^{2k}.$$

Denote by

$$J(\alpha_2, k) = \frac{1}{\alpha_n^{k+1} (2k)!!} \int_0^{+\infty} \xi_2^{2k+1} \exp\left(-\frac{\xi_2^2}{2\alpha_n}\right) \phi_{\alpha_2}(\xi_2) d\xi_2.$$

Then we can write

$$N(\alpha_2; \xi_2') = \frac{1}{\sqrt{2\pi}} \sum_{k=0}^{\infty} \frac{1}{2^k k!} \left(\frac{1 - \alpha_n}{\alpha_n} \right)^k J(\alpha_2, k) \xi_2'^{2k}. \quad (50)$$

On the other hand, the power series expansion of the exponential function gives

$$\mathcal{H}(\xi_2') \triangleq \frac{1}{\sqrt{2\pi}} \exp\left(-\frac{1}{2} \left(1 - \frac{1}{\alpha_n}\right) \xi_2'^2\right) = \frac{1}{\sqrt{2\pi}} \sum_{k=0}^{\infty} \frac{1}{k!} \left(\frac{1 - \alpha_n}{2\alpha_n} \right)^k \xi_2'^{2k}. \quad (51)$$

Secondly, we calculate $J(\alpha_2, k)$ for even α_2 . According to the formula 7.376 in Ref.[17], we have

$$J(2n, k) = \frac{(-1)^n 2^n \Gamma(n + \frac{1}{2})}{\sqrt{\pi} \sqrt{(2n)!}} F(-n, k + 1; \frac{1}{2}, \alpha_n),$$

where $n, k \in \mathbb{N}$. Here we use the Gamma function, i.e.,

$$\Gamma(n + \frac{1}{2}) = (n - \frac{1}{2})(n - \frac{3}{2}) \cdots \frac{1}{2} \sqrt{\pi}$$

and the hypergeometric function, i.e.,

$$F(-n, k+1; \frac{1}{2}, \alpha_n) = 1 + \frac{(-n)}{\frac{1}{2}} C_{k+1}^1 \alpha_n + \frac{(-n)(-n+1)}{\frac{1}{2} \frac{3}{2}} C_{k+2}^2 \alpha_n^2 + \cdots + \frac{(-1)^n n!}{\frac{1}{2} \frac{3}{2} \cdots (\frac{1}{2} + n - 1)} C_{k+n}^n \alpha_n^n,$$

where the combination number $C_{k+n}^n = (k+1) \cdots (k+n)/n!$. So we have $J(0, k) = 1$. Let $J(-2, k) = 0$. According to Gauss's recursion functions (9.137 in Ref.[17]), we have the following recursion relation about $J(2n, k)$:

$$\begin{aligned} \sqrt{(2n+1)(2n+2)} J(2n+2, k) &= (\alpha_n - 1) \sqrt{(2n)(2n-1)} J(2n-2, k) \\ &\quad + (-4n-1 + (2n+2)\alpha_n + 2k\alpha_n) J(2n, k). \end{aligned} \quad (52)$$

Then we calculate $N(\alpha_2, \xi'_2)$ by induction. Since $J(0, k) = 1$, by comparing (50) and (51), we have

$$N(0; \xi'_2) = \mathcal{H}(\xi'_2).$$

Take the derivatives about ξ'_2 in (51), and we have

$$\begin{aligned} \xi'_2 \frac{d}{d\xi'_2} \mathcal{H}(\xi'_2) &= -(1 - \frac{1}{\alpha_n}) \xi_2'^2 \mathcal{H}(\xi'_2) \\ &= \frac{1}{\sqrt{2\pi}} \sum_{k=0}^{\infty} (2k) \frac{1}{k!} \left(\frac{1 - \alpha_n}{2\alpha_n} \right)^k \xi_2'^{2k}. \end{aligned}$$

So combined with (52), we have

$$\sqrt{2} N(2; \xi'_2) = (-1 + 2\alpha_n) N(0; \xi'_2) - (\alpha_n - 1) \xi_2'^2 N(0; \xi'_2).$$

This inspires us to guess that $N(\alpha_2; \xi'_2)$ can be represented as the product of $\mathcal{H}(\xi'_2)$ and a polynomial of degree α_2 . By induction principle, assuming that for any $m \leq n$, there exist coefficients $r_{2m, 2s}$ such that

$$N(2m; \xi'_2) = \mathcal{H}(\xi'_2) \sum_{s=0}^m r_{2m, 2s} \phi_{2s}(\xi'_2), \quad (53)$$

where $\phi_{2s}(\xi'_2)$ are Hermite polynomials as in Lemma 5. Then taking the derivatives in (50) for $\alpha_2 = 2n$, we have

$$\frac{1}{\sqrt{2\pi}} \sum_{k=0}^{\infty} \frac{1}{2^k k!} \left(\frac{1 - \alpha_n}{\alpha_n} \right)^k (2k) J(2n, k) \xi_2'^{2k} = \xi_2' \frac{d}{d\xi_2'} N(2n; \xi_2').$$

Combined with the recursion relation (52) and (50), we have

$$\begin{aligned} \sqrt{(2n+1)(2n+2)} N(2n+2, \xi'_2) &= \sqrt{(2n)(2n-1)} (\alpha_n - 1) N(2n-2, \xi'_2) \\ &\quad + ((2n+2)\alpha_n - 4n - 1) N(2n, \xi'_2) + \alpha_n \xi_2' \frac{d}{d\xi_2'} N(2n; \xi'_2). \end{aligned}$$

Hence, $N(2n+2, \xi'_2)$ also has the form as in (53). Using (45), the final recursion relation of r_{α_2, β_2} is

$$\begin{aligned} &\sqrt{(2n+1)(2n+2)} \sum_{s=0}^{n+1} r_{2n+2, 2s} \phi_{2s}(\xi'_2) \\ &= \sqrt{(2n)(2n-1)} (\alpha_n - 1) \sum_{s=0}^{n-1} r_{2n-2, 2s} \phi_{2s}(\xi'_2) + ((2n+2)\alpha_n - 4n - 1) \sum_{s=0}^n r_{2n, 2s} \phi_{2s}(\xi'_2) \\ &\quad + \sum_{s=1}^n r_{2n, 2s} \sqrt{(2s)(2s-1)} \phi_{2s-2}(\xi'_2) + \sum_{s=0}^n r_{2n, 2s} (2s) \phi_{2s}(\xi'_2) \\ &\quad + (1 - \alpha_n) \sum_{s=0}^n r_{2n, 2s} \left((2s+1) \phi_{2s}(\xi'_2) + \sqrt{(2s+1)(2s+2)} \phi_{2s+2}(\xi'_2) \right). \end{aligned} \quad (54)$$

In conclusion, we have the following results: (1). $N(2n, \xi'_2)$ has the assumed form (53). (2). The recursion relation of $r_{2n, 2s}$ is given by comparing the coefficients before Hermite polynomials in (54), with the initial values $r_{-2, 2s} = 0$ and $r_{0, 2s} = \delta_{s, 0}$. (3). In particular, from (54), the coefficients $r_{2n, 2n} = (1 - \alpha_n)^n$.

References

- [1] H. Akhlaghi, E. Roohi, and S. Stefanov. A comprehensive review on micro- and nano-scale gas flow effects: Slip-jump phenomena, Knudsen paradox, thermally-driven flows, and Knudsen pumps. *Phys. Rep.*, 997:1–60, 2023.
- [2] N. Andric, D. Meyer, and P. Jenny. Data-based modeling of gas-surface interaction in rarefied gas flow simulations. *Phys. Fluids*, 31(6):067109, 2019.
- [3] C. Bardos, F. Golse, and Y. Sone. Half-space problems for the Boltzmann equation: A survey. *J. Stat. Phys.*, 124:275–300, 2006.
- [4] N. Bernhoff. On half-space problems for the linearized discrete Boltzmann equation. *Riv. Mat. Univ. Parma*, 9:73–124, 2008.
- [5] N. Bernhoff. On half-space problems for the discrete Boltzmann equation. *Il Nuovo Cimento C*, 33(1):47–54, 2010.
- [6] N. Bernhoff. On half-space problems for the weakly non-linear discrete Boltzmann equation. *Kinet. Relat. Models*, 3:195–222, 2010.
- [7] Z. Cai, R. Li, and Z. Qiao. NRxx simulation of microflows with Shakhov model. *SIAM J. Sci. Comput.*, 34(1):339–369, 2011.
- [8] B. Cao, J. Sun, M. Chen, and Z. Guo. Molecular momentum transport at fluid-solid interfaces in MEMS/NEMS: A review. *Int. J. Mol. Sci.*, 10(11):4638–4706, 2009.
- [9] C. Cercignani. *The Boltzmann Equation and Its Applications*. Springer-Verlag, 1989.
- [10] C. Cercignani and M. Lampis. Kinetic models for gas-surface interactions. *Transport Theory Statist. Phys.*, 1(2):101–114, 1971.
- [11] C. Cercignani and M. Lampis. Variational calculation of the slip coefficient and the temperature jump for arbitrary gas-surface interactions. In *Rarefied Gas Dynamics: Space-Related Studies*, pages 553–561, 1989.
- [12] T. Cowling. On the Cercignani-Lampis formula for gas-surface interactions. *J. Phys. D: Appl. Phys.*, 7(6):781, 1974.
- [13] Y. Fan, J. Li, R. Li, and Z. Qiao. Resolving Knudsen layer by high order moment expansion. *Contin. Mech. Thermodyn.*, 31(5):1313–1337, 2019.
- [14] M. Gad-el Hak, editor. *MEMS: Introduction and Fundamentals (1st ed.)*. CRC Press, 2005.
- [15] H. Grad. Note on N-dimensional Hermite polynomials. *Comm. Pure Appl. Math.*, 2(4):325–330, 1949.
- [16] H. Grad. On the kinetic theory of rarefied gases. *Comm. Pure Appl. Math.*, 2(4):331–407, 1949.
- [17] I. Gradshteyn and I. Ryzhik. *Table of Integrals, Series, and Products*. Academic Press, 2014.
- [18] E. Gross and S. Ziering. Kinetic theory of linear shear flow. *Phys. Fluids*, 1(3):215–224, 1958.
- [19] X. Gu and D. Emerson. Analysis of the slip coefficient and defect velocity in the Knudsen layer of a rarefied gas using the linearized moment equations. *Phys. Rev. E*, 81:016313, 2010.

- [20] X. Gu and D. Emerson. Linearized-moment analysis of the temperature jump and temperature defect in the Knudsen layer of a rarefied gas. *Phys. Rev. E*, 89(6):063020, 2014.
- [21] D. Hilditch. An introduction to well-posedness and free-evolution. *Int. J. Mod. Phys. A*, 28(22n23):1340015, 2013.
- [22] T. Klinc and I. Kušćer. Slip coefficients for general gas-surface interaction. *Phys. Fluids*, 15:1018–1022, 1972.
- [23] H. Kramers. On the behaviour of a gas near a wall. *Il Nuovo Cimento (1943-1954)*, 6(2):297–304, 1949.
- [24] R. Li and Y. Yang. Linear moment models to approximate Knudsen layers. *Int. J. Numer. Anal. Mod.*, 20:153–175, 2023.
- [25] R. Li and Y. Yang. On well-posed boundary conditions for the linear non-homogeneous moment equations in half-space. arXiv:2209.04629, 2022.
- [26] C. Lilley and J. Sader. Velocity gradient singularity and structure of the velocity profile in the Knudsen layer according to the Boltzmann equation. *Phys. Rev. E*, 76:026315, 2007.
- [27] S. Lorenzani. Higher order slip according to the linearized Boltzmann equation with general boundary conditions. *Philos. Trans. Royal Soc.*, 369(1944):2228–2236, 2011.
- [28] S. Loyalka. Temperature jump and thermal creep slip: Rigid sphere gas. *Phys. Fluids A*, 1(2):403–408, 1989.
- [29] S. Loyalka and J. Ferziger. Model dependence of the slip coefficient. *Phys. Fluids*, 10(8):1833–1839, 1967.
- [30] S. Loyalka, C. Siewert, and J. Thomas. Temperature-jump problem with arbitrary accommodation. *Phys. Fluids*, 21(5):854, 1978.
- [31] A. Majda and S. Osher. Initial-boundary value problems for hyperbolic equations with uniformly characteristic boundary. *Comm. Pure Appl. Math.*, 28(5):607–675, 1975.
- [32] J. Maxwell. On stresses in rarefied gases arising from inequalities of temperature. *Proc. R. Soc. Lond.*, 27(185–189):304–308, 1878.
- [33] N. Nguyen, I. Graur, P. Perrier, and S. Lorenzani. Variational derivation of thermal slip coefficients on the basis of the Boltzmann equation for hard-sphere molecules and Cercignani-Lampis boundary conditions: Comparison with experimental results. *Phys. Fluids*, 32(10):102011, 2020.
- [34] N. Sarna and M. Torrilhon. On stable wall boundary conditions for the Hermite discretization of the linearised Boltzmann equation. *J. Stat. Phys.*, 170:101–126, 2018.
- [35] F. Sharipov. Data on the velocity slip and temperature jump on a gas-solid interface. *J. Phys. Chem. Ref. Data*, 40(2):023101, 2011.
- [36] C. Siewert. Viscous-slip, thermal-slip, and temperature-jump coefficients as defined by the linearized Boltzmann equation and the Cercignani-Lampis boundary condition. *Phys. Fluids*, 15(6):1696–1701, 2003.
- [37] Y. Sone. *Molecular gas dynamics: Theory, techniques, and applications*. Birkhauser, 2007.
- [38] H. Struchtrup. Linear kinetic heat transfer: Moment equations, boundary conditions, and Knudsen layers. *Physica A*, 387(8-9):1750–1766, 2008.
- [39] H. Struchtrup. Maxwell boundary condition and velocity dependent accommodation coefficient. *Phys. Fluids*, 25(11):112001, 2013.

- [40] W. Su, Q. Li, Y. Zhang, and L. Wu. Temperature jump and Knudsen layer in rarefied molecular gas. *Phys. Fluids*, 34:032010, 2022.
- [41] W. Su, P. Wang, H. Liu, and L. Wu. Accurate and efficient computation of the Boltzmann equation for Couette flow: Influence of intermolecular potentials on Knudsen layer function and viscous slip coefficient. *J. Comput. Phys.*, 378:573–590, 2019.
- [42] P. Taheri and H. Struchtrup. Rarefaction effects in thermally-driven microflows. *Physica A*, 389:3069–3080, 2010.
- [43] P. Taheri, M. Torrilhon, and H. Struchtrup. Couette and Poiseuille microflows: Analytical solutions for regularized 13-moment equations. *Phys. Rep.*, 21:017102, 2009.
- [44] C. Tropea, A. Yarin, and J. Foss, editors. *Springer Handbook of Experimental Fluid Mechanics*. Springer-Verlag, 2007.
- [45] P. Wang, W. Su, and L. Wu. Thermal transpiration in molecular gas. *Phys. Fluids*, 32:082005, 2020.
- [46] Y. Wang and Z. Cai. Approximation of the Boltzmann collision operator based on Hermite spectral method. *J. Comput. Phys.*, 397:108815, 2019.
- [47] P. Welander. On the temperature jump in a rarefied gas. *Ark. Fys.*, 7(7):507, 1954.
- [48] M. Williams. A review of the rarefied gas dynamics theory associated with some classical problems in flow and heat transfer. *Z. Angew. Math. Phys.*, 52(3):500–516, 2001.
- [49] N. Yamanishi, Y. Matsumoto, and K. Shobatake. Multistage gas-surface interaction model for the direct simulation Monte Carlo method. *Phys. Fluids*, 11(11):3540–3552, 1999.
- [50] J. Zhang, P. Luan, J. Deng, P. Tian, and T. Liang. Theoretical derivation of slip boundary conditions for single-species gas and binary gas mixture. *Phys. Rev. E*, 104:055103, 2021.
- [51] W. Zhang, G. Meng, and X. Wei. A review on slip models for gas microflows. *Microfluid. Nanofluid.*, 13(6):845–882, 2012.